

Alma Mater Studiorum – Università di Bologna

**DOTTORATO DI RICERCA IN  
SCIENZE BIOMEDICHE**

Ciclo XXIX

**Settore Concorsuale di afferenza: 05/H1**

**Settore Scientifico disciplinare: BIO/16**

***ADVANCED IN VITRO* MODELS TO STUDY THE CROSS- TALK  
BETWEEN METASTASES AND BONE MICROENVIRONMENT:  
WHICH ROLE FOR OSTEOPOROSIS?**

**Presentata da: Melania Maglio**

**Coordinatore Dottorato:**

**Chiar.mo Prof. Lucio Ildebrando  
Cocco**

**Relatore: Chiar.mo Prof. Alberto  
Maria Martelli**

**Tutor: Dott.ssa Milena Fini**

**Esame finale anno 2017**



***“Research is to see what everybody else has seen,  
and to think what nobody else has thought”***

*Dr. Albert Szent- Gyorgyi*



# Acknowledgments

Special thanks to my tutor Dr. Milena Fini, which gave me the opportunity to follow my research activity at the Rizzoli Orthopaedic Institute, encouraging me with great enthusiasm since the first steps of my PhD course.

Thanks to my supervisor Prof. Alberto Maria Martelli, for the invaluable support in my scientific activity and unfailing care showed me through the years.

Thanks to all the researchers of the Preclinical and Surgical Studies Laboratory and of the BITTA Laboratory of the Rizzoli Orthopaedic Institute.



# Contents

## CHAPTER 1- INTRODUCTION

1.1 The bone remodeling tale.....	22
1.2 Skeletal metastases. The great migration to bone.....	27
1.3 From breast to bone: looking for the <i>congenial soil</i> .....	33
1.4 Osteoporosis.....	37
1.5 Osteoporosis and bone metastases: the dangerous liason.....	41

<b>AIM OF THE PROJECT</b> .....	45
---------------------------------	----

## CHAPTER 2 - MATERIALS AND METHODS

### **2.1 Assessment of rat bone cultures**

2.1.1 Calvaria and femoral condyle bone culture- Experimental set up .....	49
2.1.2 Assessment of bone culture viability.....	50
2.1.3 Bone culture microtomography.....	50
2.1.4 Bone culture histology.....	51
2.1.5 Statistical analysis.....	51

## **2.2 Characterization of rat breast cancer cell line (MRMT-1)**

2.2.1 MRMT-1 cells proliferation and viability.....	52
2.2.2 Wound healing assay.....	55
2.2.3 Assessment of activated pathway.....	53
2.2.3.1 Protein quantification.....	53
2.2.3.2 Western Blot.....	54
2.2.2 MRMT-1 cells sensitivity to doxorubicin .....	58
2.2.2.1 Experimental cultures set up .....	58
2.2.2.2 Evaluation of cells viability.....	58
2.2.3 Statistical analysis.....	59

## **2.3 Co-Culture of MRMT-1 cells and Osteoclasts**

2.3.1 Conditioned media preparation.....	60
2.3.2 Isolation of mononuclear cells (PBMCs) and differentiation into osteoclasts (OCs)...	60
2.3.3 PBMCs viability.....	62
2.3.4 OCs differentiation.....	62
2.3.5 OCs synthetic activity.....	62
2.3.6 Statistical analysis.....	63



**2.4 Assessment of a 3D Model of Rat Bone Metastases *In Vitro***

2.4.1 Experimental set up.....64

2.4.2 Statistical analysis.....65

**2.5 *In Vivo* Induction of Osteolytic Metastases in osteoporotic rats**

2.5.1 Surgical procedure .....66

2.5.2 Imaging evaluation of lesions development with Positron Emission Tomography (PET).....68

**CHAPTER 3- RESULTS**

3.1 Assessment of rat bone cultures.....71

3.2 Characterization of MRMT-1 cells.....76

3.3 Co-Culture of MRMT-1 cells and OCs.....82

3.4 Assessment of a 3D Model of Rat Bone Metastases *In Vitro*.....88

3.5 *In Vivo* Induction of Osteolytic Metastases in osteoporotic rats.....92

**CHAPTER 4– DISCUSSION.....94**



# List of Figures

## INTRODUCTION

Figure 1.1: The bone remodeling cycle

Figure 1.2: Histological section of sheep tibia in which the different staining of old and newly formed bone is appreciable. Fast green staining, 20x magnification.

Figure 1.3: Physiological and pathological stimuli in bone remodeling

Figure 1.4: The metastatic journey

Figure 1.5: Vicious cycle of osteolytic bone metastases

Figure 1.6: Images acquired by microCT of proximal epiphysis of tibia from a) healthy and b) osteoporotic rats

## MATERIALS AND METHODS

Figure 2.1: Experimental set up of 3D culture of calvaria segments and MRMT-1 cells

Figure 2.2: Injection of MRMT-1 cells in rat tibia through Hamilton syringe

## RESULTS

Figure 3.1: Viability trend of calvaria bone cultured up to 14 days evaluated through Alamar Blue assay

Figure 3.2: 3D reconstructions by microCT and histological images of calvaria bone segments after *in vitro* culture. Hematoxylin/Eosin staining

Figure 3.3: Viability trend of femoral condyle bones cultured up to 14 days evaluated through Alamar Blue assay

Figure 3.4: Fold change in femoral condyles mass during *in vitro* culture

Figure 3.5: Histological section of femoral condyles after 14 days of culture. Hematoxylin/Eosin staining

Figure 3.6: Microscope images of MRMT-1 cells in culture

Figure 3.7: MRMT-1 trend proliferation in different culture conditions

Figure 3.8: Results of wound healing assay: histograms graph of percentage of wound healing recovery, linear regression for assessing timing of 50% of recovery and microscope images of wound healing progression

Figure 3.9: Panel of pathways activated in MRMT-1 cell line

Figure 3.10: Doxorubicin chemical structure

Figure 3.11: Effect of different Doxorubicin concentrations on MRMT-1 cell line

Figure 3.12: Viability trend of PBMC<sub>OVX</sub> and PBMC<sub>SHAM</sub> in CTR-, CTR+, CM-, CM+ and TW culture conditions at one and two weeks

Figure 3.13: TRAP staining images of PBMC<sub>OVX</sub> and PBMC<sub>SHAM</sub> in CTR-, CTR+, CM-, CM+ and TW culture conditions at one and two weeks [Salamanna et al, 2016]

Figure. 3.14: Protein content of PBMC<sub>OVX</sub> and PBMC<sub>SHAM</sub> in CTR-, CTR+, CM-, CM+ and TW culture conditions at one and two weeks [Salamanna et al, 2016]

Figure 3.15: Box plot graph of viability values distribution of SHAM, OVX, SHAM+MRMT-1 and OVX+MRMT-1 groups at 7 and 14 days of culture

Figure 3.16: Viability trend of SHAM, OVX, SHAM+MRMT-1 and OVX+MRMT-1 groups at 7 and 14 days of culture

Figure 3.17: Western blot of MRMT-1 protein content after sham and osteoporotic culture

Figure 3.18: Histological images of calvaria segments after culture with MRMT-1 cells. Hematoxylin/Eosin staining

Figure 3.19: Biological parameters and microPET analysis results of Sham and Ovx rats



# List of Abbreviations

BMU- Basic Multicellular Unit

OCs- Osteoclasts

OBs- Osteoblasts

Ca- Calcium

IL- Interleukin

TNF- $\alpha$ - Tumor Necrosis Factor  $\alpha$

IGF- Insulin like Growth Factor

CSF- Colony Stimulating Factor

EGF- Epidermal Growth Factor

PDGF- Platelet Derived Growth factor

ALP- Alkaline Phosphatase

COLLI- Type I Collagen

OC- Osteocalcin

OP- Osteopontin

ON- Osteonectin

DMP1- Dentin matrix acidic phosphoprotein 1

FGF- Fibroblast Growth Factor

RANKL- Receptor activator of nuclear factor kappa-B ligand

OPG- Osteoprotegerin

RANK- Receptor activator of nuclear factor kappa-B

EPH- ephrinB2

EphB4- protein ephrinB2 receptor B4

S1P- sphingosine 1- phosphate

VEGF- Vascular Endothelial Growth Factors

TGF-  $\beta$ - Transforming Growth Factor  $\beta$

BMP- Bone Morphogenetic Protein

HIF- 1- Hypoxia Induced- Factor

EMT- Epithelial To Mesenchymal Transition

VEGFR- Vascular Endothelial Growth Factors receptor

ECM- Extracellular matrix

CTS- Cathepsin

MMP- Metalloproteinase

DKK1- Dickkopf-related protein 1

ErbB2- Human Epidermal Growth Factor Receptor 2

CXCR4- C-X-C Chemokine Receptor Type 4



SDF1/CXCL12- Chemokine Stromal Cell Derived Factor-1

IHH- Indian Hedgehog

PTHrP- Parathyroid hormone-related protein

PGE2- Prostaglandin

ER  $\alpha$  - Estrogen Receptor  $\alpha$

OP- Osteoporosis

BMD- Bone Mineral Density

SD- standard deviation

Vit.D- Vitamin D

VDR- Vitamin D Receptor gene

CYP2R1- Vitamin D 25-hydroxylase gene

NF-  $\kappa$ B -Nuclear Factor kappa-light-chain-enhancer of activated B cells

BCAR1- Breast cancer anti-estrogen resistance protein 1

TRAF- TNF receptor-associated factor

FSH- Follicle-Stimulating Hormone

CTGF- Connective Tissue Growth Factor

BMSCs- Bone Marrow Stromal Cells

PBMCs- Peripheral Blood Mononuclear Cells

3D- Tridimensional

RPMI- Roswell Park Memorial Institute

BSA- Bovine Serum Albumine

DMEM- Dulbecco's Modified Eagle Medium

FBS- Fetal Bovine Serum

°C- Celsius

MicroCT- Microtomography

SDS-PAGE- Polyacrylamide Gel in Sodium Dodecyl Sulphate

GLB- Gold Lysis Buffer

AKT- Protein Kinase B

PKR- Protein kinase RNA-activated

SHAM- Healthy

OVX- Ovariectomized

FCS- Fetal Calf Serum

TRAP- Tartrate-Resistant Acid Phosphatase

RGB- Red- Green- Blu

PET- Positron Emission Tomography

<sup>18</sup>F-FDG- <sup>18</sup>F-Fluorodeoxyglucose

EGFR- Epidermal Growth Factor Receptor

PTEN- Phosphatase and tensin homolog

S6RP- Phosphorylated S6 ribosomal protein

Bcl2- B-cell lymphoma 2

Bcl- XLB-cell lymphoma-extra large



# **CHAPTER 1-**

# **INTRODUCTION**

## 1.1 THE BONE REMODELING TALE

Under the deceptive appearance of a static tissue, bone hides a complex remodeling system which is the base of its unique properties. The classical study of bone remodeling arguably takes its first steps from a work of 1969 by Harold M. Frost [*Frost et al, 1969*], which outlined the main actors and key passages of the process through the use of tetracycline labeling. Particularly remarkable it is the introduction of the–“*Basic Multicellular Unit*” (BMU), intended as the set of cellular components – osteoclasts (OCs), osteoblasts (OBs) and osteocytes- involved in the remodeling process, which is in turn described as a cycle as portrayed below:

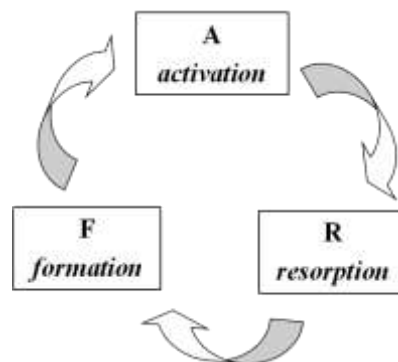


*Figure 1.1: The bone remodeling cycle*

Indeed, it is now well known that bone turnover is a well- balanced fluctuation between degradation of pre- existing tissue by OCs (resorption) and replacement with newly- formed one through OBs activity (formation). [*Adachi et al, 2009*] (**Figure 1.2**)

The phase of activation is related to both a systemic and local metabolic activity, usually in response to mechanical loading and microfractures (whose cellular mediators, the osteocytes, are involved in the mechanism of mechanotransduction) [*Adachi et al, 2009*] but also taking

part to the homeostasis of serum calcium ( $\text{Ca}^+$ ) and minerals concentration. [*Raisz et al, 1999; Henriksen et al, 2009*]

Apart from lifestyles, diet, genetic factors and microenvironment, under physiological conditions, there are many local and systemic factors which can control and regulate bone remodeling: classical cytokines and growth factors are Interleukins (IL) like IL-1, 6, 9, 10, Tumour Necrosis Factor  $\alpha$  (TNF- $\alpha$ ) 1 and 2, Insulin like Growth Factor (IGF) I and II, Colony Stimulating Factor (CSF), Epidermal Growth Factor (EGF), Platelet Derived Growth factor (PDGF). [*Hadjidakis et al, 2006*]

The mechanism of bone regulation starts also from molecules expressed primarily by the bone cells involved in the process. Alkaline Phosphatase (ALP), Type I Collagen (COLLI), Osteocalcin (OC), Osteopontin (OP) and Osteonectin (ON), key regulators in bone matrix synthesis and mineralization, are expressed by mature OBs whose differentiation is in turn stimulated by Wnt signaling pathway, also involved in OCs maturation. The life cycle of OBs is closed by their transformation in osteocytes, which act on bone formation through the expression of, namely, Dentin Matrix Acidic Phosphoprotein 1 (DMP1), Fibroblast Growth Factor (FGF) 23 and Sclerostin. [*Eiksen et al, 2010*]

A key role is played by the system of Receptor activator of nuclear factor kappa-B ligand (RANKL) and its decoy receptor Osteoprotegerin (OPG). RANKL (member of TNFs family) is expressed by OBs and stromal cells and induce OCs formation via binding the Receptor activator of nuclear factor kappa-B (RANK), which is in turn expressed by pre- OCs, B and T cells, dendritic cells and fibroblasts. The binding between RANKL/RANK stimulates OCs activation and survival, promoting also their adhesion to the bone and their osteolytic activity. These activities are inhibited by OPG, expressed by OBs and bone marrow cells, via apoptosis of OCs. [*Khosla et al, 2001*] (*Figure 1.3*)

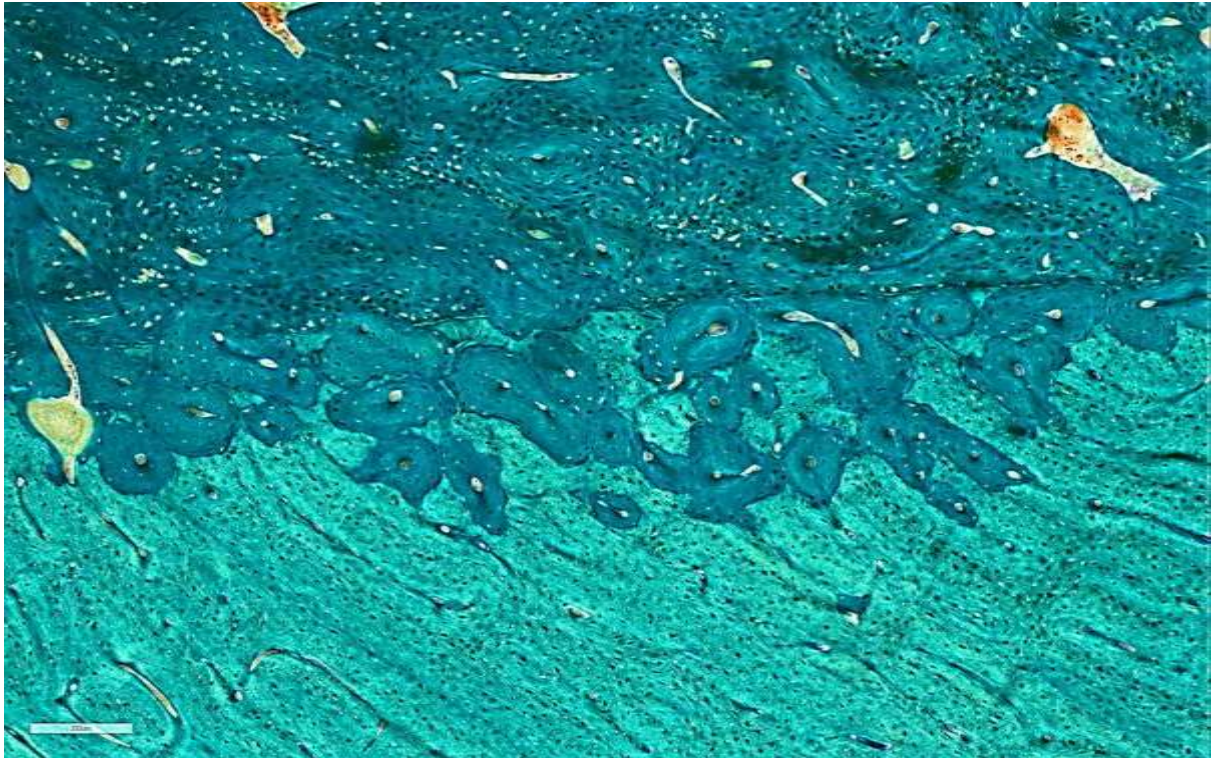


*Figure 1.2: Histological section of sheep tibia in which the different staining of old and newly formed bone is appreciable. Fast green staining, 20x magnification.*

The coupling activity of OCs and OBs in regulation of bone remodeling is also highlighted by the presence of other cross talks, like the one between the transmembrane protein EphrinB2 (EPH) and its receptor B4 (EphB4), expressed respectively on OBs and OCs. In this pathway it is also involved the Sphingosine 1- Phosphate (S1P), which, when secreted by OCs, activates EphB4 signaling, promoting OBs differentiation and inhibiting OCs activity.

**[Ryu et al, 2006].**

Among the elevated metabolic activity, another important feature of bone is being a highly vascularized tissue. Vascularization represents a critical step in the phase of bone remodeling, as suggested by its indefeasibility, during the development of human organism, in the correct endochondral ossification, in which blood vessels spread through the cartilaginous matrix, mediated by the Vascular Endothelial Growth Factors (VEGF), promotes and sustains bone formation. VEGF surely plays a pivotal role in angiogenesis and neovascularization; its



activity in the bone tissue is intuitive when considering that many factors involved in bone remodeling, including mechanical stress, are also responsible for the control of the synthesis and activity of VEGF, namely the transcription factor Osterix, growth factors like Transforming Growth Factor  $\beta$  (TGF- $\beta$ ) and FGF 2, inflammatory cytokines like IL-1, 6 and 8, Prostaglandin E1 and 2, Bone Morphogenetic Protein (BMP), mostly expressed by cell of osteoblastic lineage [*Hu et al, 2016*].

Although the mechanisms that regulate the role of angiogenesis in bone remodeling have not yet been put fully into focus, it is more and more evident that the link between angiogenesis and osteogenesis lives in the hypoxic environment which characterizes the bone tissue. In fact under hypoxic condition OBs, as well as tumor cells, are stimulated to express the hypoxia induced- factor (HIF-1 alfa), transcription factor which promote VEGF-A mRNA expression, augmenting among angiogenesis also bone formation. This feature appears particularly interesting when considering it is shared with cancer, marking a first point in the affinity between tumor cells and bone. [*Schipani et al, 2009*]

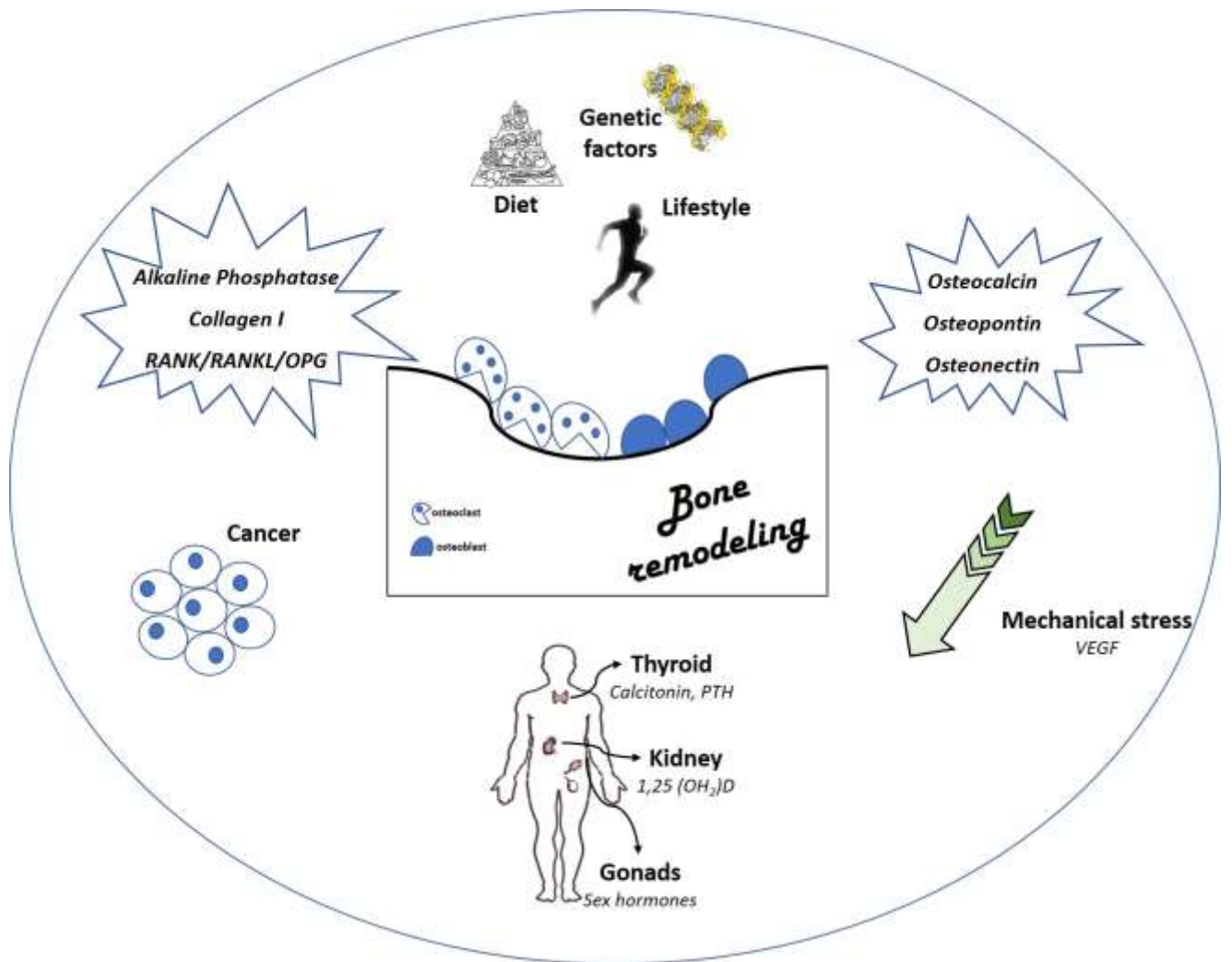


Figure 1.3: Physiological and pathological stimuli in bone remodeling

## 1.2 SKELETAL METASTASES. THE GREAT MIGRATION TO BONE

The skeleton is the organ more frequently affected by metastases, especially from breast and prostate cancers, whom it is possible to attribute almost the 80% of all bone metastatic diseases; this reflects both the high incidence that the relatively long clinical course of these tumors. Among breast and prostate, even other several common solid tumors, such as tyroide, lung and kidney cancers show tropism for the bone, although with a lower incidence. [*Buijs et al, 2009*]

Bone metastases have been commonly classified for a long time as osteolytic or osteoblastic, depending on whether the detected alteration was an excessive loss or apposition of bone. The morbidity and the complications associated with metastatic bone disease, like bone pain, pathologic fractures, spinal cord compression, leukoerythroblastic anemia, bone deformity and hypercalcemia, impair significantly patients' quality of life. [*Roodman et al, 2004*]

In metastatic patients, long term survival dramatically decreases, and treatments are mostly palliative; among these, surgery still remains the gold standard, often associated with chemotherapy, radiotherapy, therapies with drugs acting on bone remodeling (i.e. biphosphonates), hormonal therapy, thermal ablation and electrochemotherapy [*Coleman et al, 2010*]

Although the understanding of the precise mechanisms regulating the predilection of some cancers to bone remains still incomplete, it is now increasingly being recognized that the unique characteristics of the bone microenvironment provide signals that lead to a selective growth advantage for cancer cells and, probably, the resistance to some therapeutic treatments.

However, the study of more effective therapies and the understanding of the underlying mechanisms of tumor escape and resistance to drugs is still an open field. In the last years,

the results highlighting the influence that microenvironment exerts on tumor cells behavior have brought out new scenarios of complexity, from the onset of cancer to metastatic process. It is now clear that the heterogeneity of metastatic patterns is related to the biological cellular and molecular features of both starting cancer cells and metastasized tissues and also the traditional classification of metastases in osteolytic and osteoblastic seems to be overcome by the evidence of “mixed” metastatic lesions, with hallmarks common to both groups. This reflects the two extremes of a continuous spectrum of changes in bone remodeling during the development of metastasis. [Coleman, 2001]

Several hypotheses have been discussed to speculate the mechanism driving cells from primary tumor to bone, attributing to different factors and conditions some “attractive” properties which might clarify the tropism to the bone.

The multistep process that lead cancer cells towards the road to bone is characterized by the ability of cells to adapt, surviving in many different conditions, and by the affinity that they show for the target organ. (Figure 1.4)

This kind of similarity can be expressed in terms of osteomimetic abilities more than capability to secrete proteins or express genes suitable for bone colonization. The first and more iconic step in this long route is the *epithelial to mesenchymal transition* (EMT), to which cancer cells undergo in the passage to bloodstream. This transformation, which seemed at first to be the starting point of the metastatic process, actually is more and more recognized as the double face of the same item. In fact, the capability of cancer cells to disseminate and metastasize far away from the primary tumor is marked by the loss of some proteins related to cell-cell junctions and which are typical markers of epithelial cells, namely E-cadherin and cytokeratin. On the other hand, this phenomenon is subverted once reached the target organ, considering that the ability to invade and colonize is mediated by the expression of proteins

characteristics of epithelial cells, and to this end, it occurs the reverted transition named *mesenchymal-to-epithelial transition*. [Kan et al, 2016]

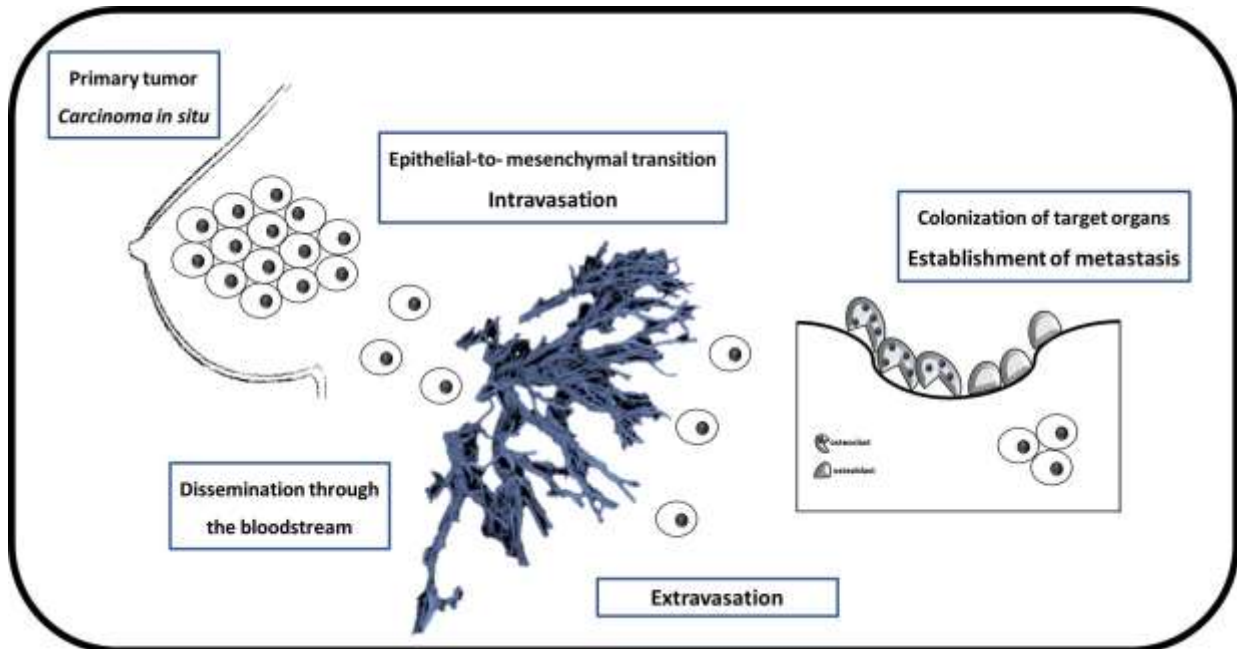


Figure 1.4: The metastatic journey

Surely, once in the vascular bed, cancer cells can find stimuli driven by factors involved in the various aspects of bone remodeling, namely angiogenesis, minerals release (primary Ca) and high concentrations of growth factors. [Gupta et al, 2006] Some factors are then related to the peculiar characteristics of bone microenvironment, such as low oxygen level and acid pH, which can create a favorable environment for cancer cells colonization and onset of metastases. [Kingsley et al, 2007] The pivotal role of vascular component and blood flow anatomy in this framework is indicated by the preference of cancer cells to metastatize to high-vascularized bone district, such as bone marrow of long bones, pelvis, sternum, ribs and vertebrae.

Studies on animals and on cadavers have shown an involvement of the vertebral venous plexus that could help to explain the tropism of these tumors to the bone. In fact, the venous blood coming from the pelvis and from the breast not only flows into the vena cava, but also directly into the vertebral venous plexus, especially in condition of high intrathoracic or intraddominal pressure. *[Kaplan et al, 2006]* The tropism for bone containing red marrow seems to have found another explanation in the studies on the relationship between the metastatic cells and the hematopoietic progenitor cells present in the bone marrow. In fact, the combination of chemotactic and adhesion molecules in the endothelium of bone marrow has proved to be particularly favorable to colonization by cancer cells. Recent studies have shown that after about two weeks after implantation of the primary tumor, and before the invasion phase, hematopoietic stem cells expressing the receptor for VEGF (VEGFR-1) are organized to define the contours of what will be the site of metastasis. This structure, called "pre-metastatic niche", works as a physiological niche, in which the VEGFR-1 + cells can maintain the expression of stem cell markers (c-kit, CD34) without differentiating. The signal mediated by VEGF is a critical factor because it stimulates angiogenesis, the growth of the primary tumor and of the metastasis dormant activity. In addition, the VEGFR can induce MET and tumor invasion. *[Kaplan et al, 2005]*

Finally, it is known that cancer cells can form emboli, which remain blocked in the capillaries beds within the bones. Once the clot or the cancer cells have reached the skeleton, the features of the microenvironment favor its survival. Hypoxia is a hallmark of all solid tumors, whose rapid proliferation prevents adequate angiogenesis and thus a complete perfusion. The hypoxic microenvironment in the bone marrow regulates hematopoiesis. The cells that metastasize to the bone not only are able to survive in low amounts of oxygen, but also are further advantaged, both in terms of proliferation and in terms of resistance to radio / chemotherapy treatments.

The presence of an acid environment also seems to promote the establishment of metastases. Extracellular pH exerts an important effect in bone remodeling, and in this sense, is carefully regulated, leading to an increase in the formation of resorption pit and at the same time to a reduced OBs mineralization and bone formation.

The influence of pH is so pronounced that even a mild but chronic acidosis can strongly stimulates osteoclasts activity up to cause a marked bone loss. [Arnett, 2003] The link between condition of acidosis and tumor invasion seems to live in the alteration of glycolytic metabolism, which characterize many tumors. In fact, even in presence of oxygen, cancer cells exhibit reduced glycolytic pathway, that with lactic acid production and lower pH, give them a more aggressive phenotype and increase their proliferation. Differently, in the same condition of acid- mediated toxicity, normal cells undergo to necrosis and apoptosis, devoiding of the adaptability of cancer cells. At the same time, acid microenvironment leads to extracellular matrix (ECM) degradation and release of Cathepsin B (CTSB), metalloproteinase (MMP) and other proteolytic enzymes with contribute to metastases onset. [Gatenby et al, 2006].

Once invaded bone, cancer cells start to interact with resident cell populations, as bone cells, hematopoietic stem cells and so on, expressing osteomimetic factors and adhesion molecules so modifying their genotypic and phenotypic profile. These changes might be induced by the interaction with the new microenvironment, whose mineral component makes bone surface five or six times harder than those of soft tissues and consequently more resistant to the action of proteolytic enzymes secreted by tumor cells. [Coleman et al, 2010]

The adhesive interaction with bone matrix and medullar stroma trigger cancer cells to produce angiogenic factors and resorptive molecules that further promote tumor growth.

It is more and more evident that the development, more than the onset of bone metastases, seems to be influenced by the state of bone metabolism. Study conducted on the influence of

ovariectomy on the establishment of bone metastases in a mouse model didn't evidenced any difference with sham group in terms of migration of cancer cells to the metastatic site; however, interestingly, cell colonization seemed to be enhanced in osteoporotic environment, with an increase in the expression of genes involved in metastatic spread such as RANKL, Dickkopf-related protein 1 (DKK-1), MMP- 9 and Cathepsin K. Specularly, the same trend can be observed in mice undergone to orchietomy, with an increased aggressiveness in tumor behavior, secondary to a more intense osteoclastic resorptive activity. [*Kan C et al, 2016*]



### **1.3 FROM BREAST TO BONE: LOOKING FOR THE “CONGENIAL SOIL”**

Breast cancer represents one of the primary tumor that more frequently metastatize to bone, with almost the 70% of patients affected by this type of tumor showing distant skeletal metastatic lesions. For a long time metastases from breast cancer have been classified as osteolytic but now it is increasingly recognized that the old dichotomy between osteolytic and osteoblastic metastases has no more reason to be, as bone metastatic lesions frequently shows mixed signs of unbalanced activities of bone resorption and formation.

The first attempt to find an explanation to the preferential harbor of some site to cancer cells, dates back to nineteenth century, with the study of Ernst Fuchs on the metastatic pattern of uveal melanoma; he first advanced the hypothesis that the metastatic process was not consequence of casualty but of some predispositions of both sites of start and arrival.

Thanks to the inspiration drown by this first suggestion, Stephen Paget started his systematic work that will be resulted in the formulation of the theory known as of “*Seed and soil*” [Paget, 1889]. In the 1889, after the autoptic evaluation of 735 cases of breast cancer with fatal outcome, he hypothesized that the colonization of an organ or a tissue by cancer cells is the result of the productive mutual interaction between tumor cells and the host microenvironment, with the famous claim “*When a plant goes to seed, its seeds are carried in all directions; but they can only grow if they fall in congenial soil*”.

A great input for breast cancer cells to head to bone is given by the high expression of molecules promoting the invasion and adhesion to the bone tissue, including the receptor tyrosine kinase ErbB2 (Human Epidermal Growth Factor Receptor 2), frequently amplified, which in turn stimulates the expression of CXCR4 (C-X-C Chemokine Receptor Type 4) increasing protein synthesis and inhibiting its degradation. The proliferation and migration of cancer cells is then stimulated by the strengthening of pathways SDF1/CXCL12 (Chemokine Stromal Cell Derived Factor-1), which also promotes angiogenesis by recruiting endothelial

cells. Once in the bone, the SDF1 expressed in specific vascular microdomains can promote transendothelial migration of breast cancer cells expressing CXCR4. The presence of CXCR4 + cells, once in the bone marrow, in synergy with RANKL, can further stimulate cell migration in response to SDF1 and RANK, locally produced. The integrin  $\alpha\beta3$ , finally, allows the adhesion of cancer cells to the components of the bone matrix, thus promoting the development of osteolytic metastases [*Rose et al, 2006*]

A possible relationship between the metastatic tumor cells and stromal cells and OBs present at bone level can be found in the common expression of Cadherin 11, involved in the homophilic cell-cell interactions. It is believed that the preferential migration of breast cancer cells in the bone is due to the interactions mediated by cadherin between the two cell populations. It also seems to be involved in the formation of metastases, enhancing osteoclastogenesis [*Tamura et al, 2008*]

Finally, a pattern to describe bone remodeling in the presence of cancer cells was introduced in the early '90s and has been called "*the vicious cycle of bone metastases*" [*Chen et al, 2010*]. It has been suggested that cancer cells metastatize and are then able to live and proliferate preferentially in the bone, thanks to their ability to express factors generally considered related to the bone. It is interesting that most of these osteomimetic factors are modulated by the same transcription factor, Runx2, considered being the key regulator in the commitment and differentiation of OBs. Runx-2 seems to respond to stimulation of the TGF- $\beta$  activating the expression of Indian Hedgehog (IHH); this pathway, which also involves the cascade of Mitogen-Activate Protein Kinase (MAPK), leads to an increased osteoclastogenesis and osteolysis. [*Hansen et al, 2007*]

In the vicious cycle of bone metastases, bone destruction increases local levels of Ca, promoting tumor growth and the production of Parathyroid hormone-related protein (PTHrP). Breast cancer cells produce, or induce, IL-1, IL-6, IL-8, IL-11, Prostaglandin (PGE<sub>2</sub>), M-

CSF, TNF- $\alpha$ , which stimulate OCs formation, activation and migration. In particular, IL-8 may indirectly promote osteoclastogenesis by regulating positively the expression of RANKL on osteoblastic precursors. Conversely, the IL-11 promotes the maturation of OBs from mesenchymal progenitor cells. [Yin *et al*, 2005] Taken together, these data suggest that PTHrP is the principal mediator of secondary osteolytic lesions in breast cancer and other solid cancers [Rose *et al*, 2006] (Figure 1.5)

As inferred from the nature of the osteolytic process, the bone microenvironment contains many proteases and, among these, the MMP family, made up of more than twenty zinc-dependent proteases, can degrade all components of the ECM. Tumor cells, OBs, OCs and endothelial cells produce MMPs [Chen *et al*, 2010] whose expression is regulated by the levels of TGF- $\beta$  and TNF- $\alpha$ . MMPs, and in particular the protease D, contribute to the proteolysis of collagen from the surface of osteoid before the attack of osteoclasts, facilitating the metastatic invasion through the removal of this physical barrier. [Gall *et al*, 2007]

As part of the breast carcinomas an important role is played by the presence of Estrogen Receptor  $\alpha$  (ER  $\alpha$ ), being estrogens mitogenic to the cancer cells. Some studies suggest that TGF- $\beta$  promotes the transcription mediated by the ER receptors which in turn stimulate the production of PTHrP and should thus have a role in the development and progression of metastatic breast cancer to bone [Chen *et al*, 2010]

Tumor progression, however, is also critically controlled by angiogenesis. OCs are adjacent to blood vessels growing in the Havers channels; metastases from breast cancer strongly express VEGF, and OCs express both VEGFR1 that VEGFR2. VEGF can promote osteoclastogenesis and the C-terminal region of the PTHrP may induce the expression of VEGF in bone cells. In addition, the VEGF can interact with monocytes to induce the differentiation into OCs [Kaplan *et al*, 2006].

In parallel to osteolytic lesions, there is a modulation of the function of OBs that induces necrosis and apoptosis. This is mediated by the production, by tumor cells, of IL-1, IL-11, TNF- $\alpha$  and, especially, of Fas ligand (FasL) which, interacting with its receptor Fas, expressed by OBs, activates caspases pathway.

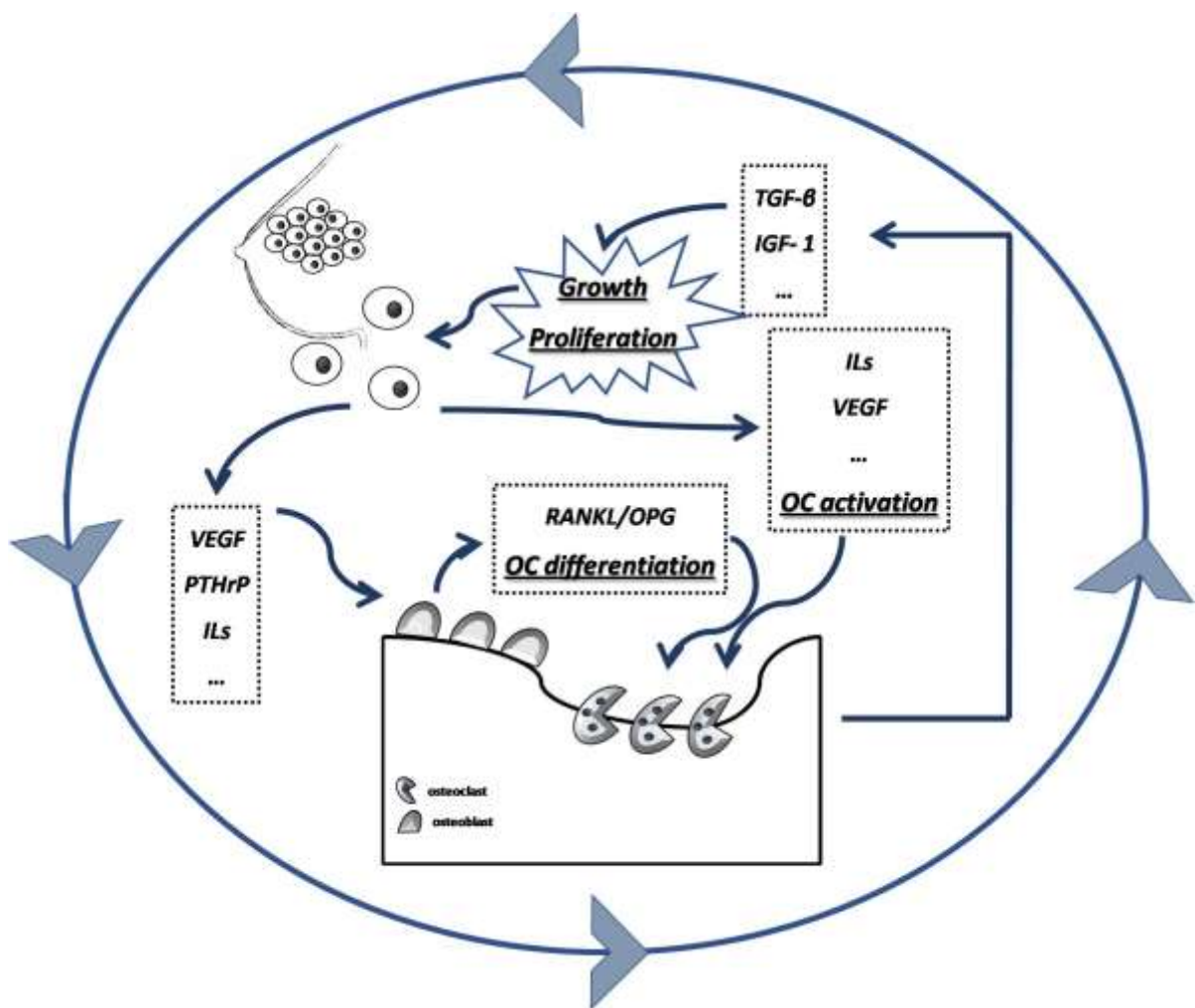


Figure 1.5: Vicious cycle of osteolytic bone metastases

## 1.4 OSTEOPOROSIS

It dates back to 1820 the appearance of the term “osteoporosis” (OP) to indicate a generic state of pathological alteration of bone. [Schapira D et al, 1992] Since then, many have been the attempts to find an exhaustive definition of OP, but the effort is challenging considering the manifold aspects emerging by the study of etiology and characteristics of this pathology. OP can be defined as a systemic disease affecting bone, clinically identified by a value of Bone Mineral Density (BMD) deviating of at least 2.5 standard deviation (SD) from the mean value of general healthy population (T score  $<-2.5$  SD). Despite this clinical evidence, if it is true that people with such value of BMD are affected by OP, it's not true the contrary, as not only the course of the condition can remain asymptomatic until the occurrence of the first fracture, but also many patients can suffer from a severe subverted skeletal condition while having a normal BMD index. These observations give reason of the difficulty of setting OP in a well-defined framework. [Salamanna et al, 2015]

The conventional classification of osteoporosis identify mainly two groups:

- primary OP, which assembles OP which occurs after establishment of menopause and the one related to advanced age, affecting the 30% of women;
- secondary OP, which is related to external factors, like unhealthy lifestyles and diet (excessive assumption of alcohol or fat, lack of physical activity, smoking or reduced exposure to sunlight) or to other pathological conditions which can directly or indirectly affect bone, involving between the 30% and 60% of male, and more than 50% of woman.

[Fini et al, 2012]

Among this classical division, it must be considered OP as a more heterogeneous pathology, in whose pathogenesis are also involved genetic factors, which evidence increases the level of complexity, adding to the various variables also the individual predisposition. In recent years more and more attention has been given to Vitamin D (Vit.D) and to the mutation that can

occur in genes involved in the related regulation pathways. Some studies in fact found a correlation between polymorphisms in vitamin D pathway genes, in particular in the gene encoding for Vit.D receptor (*VDR*) and onset of OP, ascribing to it a connection with lower BMD and consequent development of OP. Polymorphisms of the gene encoding for Vit.D 25-hydroxylase (*CYP2R1*) are proposed to correlate with alteration in Vit. D metabolism and consequent insufficient levels of Vit.D. This aspect appears particularly intriguing considering that low levels of Vit. D correlate with stimulation of immune system in terms of release of pro inflammatory molecules, TNF- $\alpha$ , resistin, and free fatty acids, and of activation of Toll-like receptors. In the light of the fact that OP can be considered a state of chronic inflammation, alteration of *CYP2R1* seems to indirectly promote the osteoporotic condition.

*[Bellavia et al, 2016]*

OP has nowadays settled as one of the most relevant pathological conditions, being estimated to be cause over the next ten years of at least 3 million of fracture/year and to charge more than \$25 billion/year to the health system. The evidence of the extent of the issue has lead to the launch of extensive screening programs to monitor and prevent the morbidity associated and the design of clinical trial to deal with the establishment of the pathology. Considering the relevance that this pathology has assumed in terms of impact on public health and costs for assistance, it could sound strange that the first evidence of the link between menopause and osteoporosis dates back to less than a century. Fuller Albright seems to hold the notable credit for identifying first the possible correlation between the onset of OP and endocrine state *[Albright et al, 1940]*, while a milestone in the classification of various type of OP, different for etiological factors, can be found in the paper by Riggs et al which advanced the so called “Unitary Model for Involutional Osteoporosis”. In this work in particular, starting from the assumption that in the absence of other kinds of pathologies bone remodeling remains quite balanced up to middle age, bone loss consequent to menopause and lowering of

estrogen levels is described as a process articulated in two phases: the first one defined “fast”, characterized by marked bone loss and in particular of trabecular bone, with a ratio between trabecular and cortical bone loss of 3:1. The second phase, which can be considered common to male and female gender, is “slow” and more balanced, with a ratio of 1:1 in terms of loss between the two types of bone. [Riggs *et al*, 1983] It has been estimated that within the first ten years from the establishment of OP, at least  $\frac{1}{4}$  of the mass of trabecular bone can be lost in woman during the “fast” phase. (Figure 1.6)

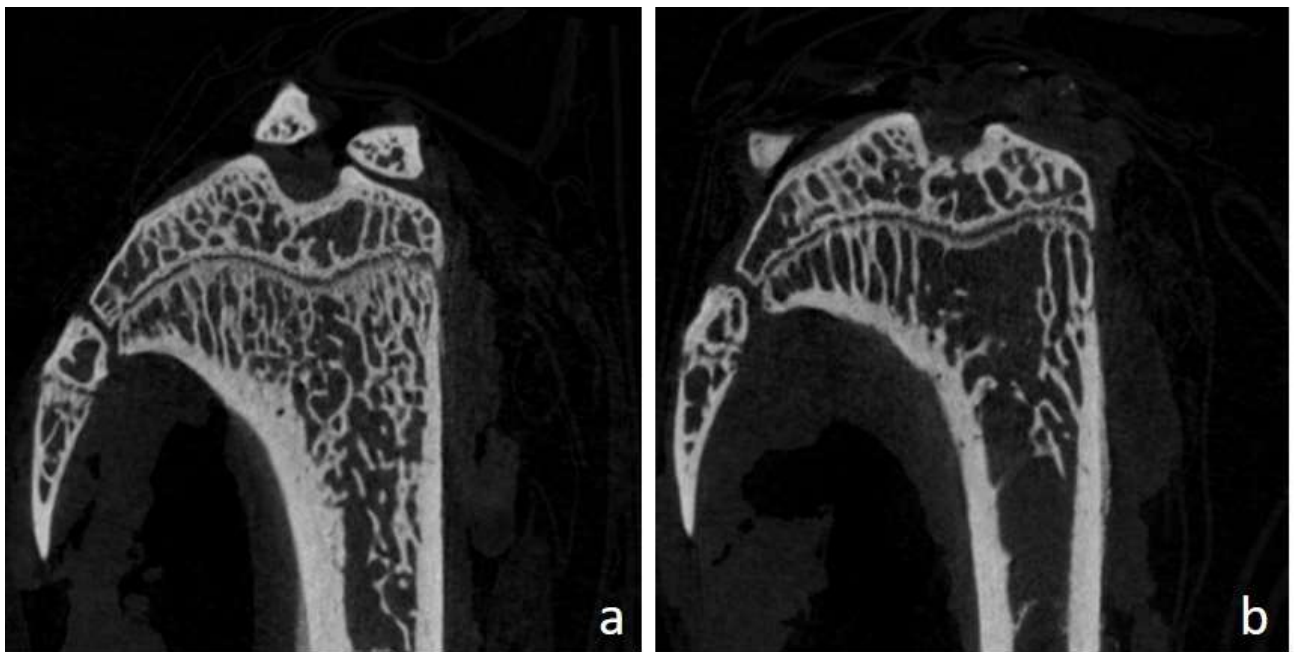


*Figure 1.6: Images acquired by microCT of proximal epiphysis of tibia from  
a) healthy and b) osteoporotic rats.*

The influence of estrogens in bone development and remodeling is common to lots of species, included rodents and humans, both in female and in male, even though all the aspects of this regulation have not been fully elucidated. Some papers suggest that the primary action of estrogens is not realized in the bone microenvironment but at the level of other targets which in turn exert an osteoprotective activity. For example, in the frame of the negative

feedback regulating follicle-stimulating hormone (FSH) physiological levels, estrogens increase the production of IGF-1 in liver, which has also the effect of enhancing OBs bone deposition. [*Imai et al, Mol Endocrinol 2010*] Estrogens can also act directly on bone remodeling exerting their actions on bone cells populations, in particular preventing OCs formation. This action is performed interfering with the Nuclear Factor kappa-light-chain-enhancer of activated B cells (NF- $\kappa$ B) /RANKL pathway, via the formation of the complex of ER $\alpha$  with the scaffolding protein Breast cancer anti-estrogen resistance protein 1 (BCAR1), which sequester TNF receptor-associated factor 6 (TRAF6) and prevent monocytes to differentiate into OCs. In addition, estrogens play a role in the activation of bone resorption via inhibition of OBs apoptosis induced by DNA damage and through phosphorylation of Src/Shc/ERK pathway. [*Faienza et al, 2013; Imai et al, 2010*].

Furthermore, it is more and more evident that the number and the function of ER $\alpha$ , expressed by cells of osteogenic lineage and, obviously, estrogen levels in human body, influence bone homeostasis in terms of adaptation to mechanical stress. After all, presence of ERs has been detected during bone callus formation, underlining the role in bone remodeling related to mechanical stress [*Zaman et al, 2006*].



## 1.5 OSTEOPOROSIS AND BONE METASTASES: THE DANGEROUS LIASON

One of the most important feature of the bone microenvironment is its sensitivity to the changes exerted by the endocrine system, as bone cells suffer any oscillation in hormones production. In this framework, osteoporotic condition can be considered a possible actor in the onset of metastatic disease, being correlated to the hormonal derangement secondary to the establishment of menopause, with all the possible consequence on bone homeostasis. In fact, in condition of normal production of sexual hormones and in particular in physiological estrogenic condition, the inflammatory state and cytokines production results to be regulated via the inhibition of T-cells. The existence of this control system, aimed to monitor OCs activation and the rate of bone remodeling, is meaningful of the upheaval in bone metabolism in the presence of a state of OP, in which the vertical drop of estrogen levels activates the RANK/RANKL pathway, stimulating bone resorption more than formation, along with lowering OPG levels.

Inflammation in fact is one of the key characteristic of osteoporotic condition, related to the increased bone resorption and consequent osteolysis. [Wu YP *et al*, 2010] Osteolysis in fact leads to an augmented release of cytokines, like TGF- $\beta$ , which in turn stimulates the transcription of IL-11 and of genes related to extracellular matrix, like the Connective Tissue Growth Factor (CTGF), which potentiate the metastatic progression. [Kozlow *et al*, 2005]. In addition, the enhanced bone resorption creates a favorable microenvironment for the metastatic arrangement even thanks to the action of many growth factors, namely TGF- $\beta$ , IGF, FGF, PDGF, which are released during osteolysis. [Wright *et al*, 2014]

Among the ways in which the state of chronic inflammation in OP influence the metastatic process, making it easier, a pivotal role is played by the ensuring greater passage through the bloodstream, via the impairment of blood vessels integrity. [Wu YP *et al*, 2010]

In addition, angiogenesis, which is a well-recognized essential element for establishment of metastases, finds an enhancer both in the action of proteolytic enzymes derived from OCs and in the increased expression of leptin typical in the osteoporotic condition, in which fat mass tends to increase. Leptin, in fact, stimulates VEGF expression and consequently blood vessels growth, and seems to act on proto-oncogene tyrosine-protein kinase Src and integrin  $\alpha(v)\beta 5$ , which in turn act on circulating angiogenic cells. In addition, there are more and more evidence about the influence exerted by leptin on bone metabolism and in particular on bone cell populations. In fact, on the one hand, OBs and chondrocytes are affected by leptin via the expression of the signaling form of its receptor. On the other hand, leptin is involved also in the pathway regulating RANK and RANKL and so influencing OCs differentiation, and also acting positively on the number of bone marrow stromal cells (BMSCs) and peripheral blood mononuclear cells (PBMCs). *[Reid, 2008]*

The correlation between OP and onset of bone metastases has stimulated a new field in the research of novel reliable markers for early diagnosis of metastatic disease development and for the identification of new therapeutic targets.

Evidences of the fact that alterations in bone status can affect the fate of metastatic cancer cells have emerged in the first instance probably from clinical studies, testing pharmacological treatment for OP and evidencing differences between pre- and post-menopausal subjects. The picture that emerges still remains complex, underlining that, if it is true that anti resorptive drugs demonstrated to have an inhibitor effect on the spread of metastatic disease, on the other hand metastases can occur years after the eradication of primary tumor and in older subject with a possible already reverted bone metabolism due to OP.

Ottewil et al, with their pioneeristic work with xenogenic model of osteoporotic mice, demonstrated first that bone microenvironment altered by OP is more receptive for cancer

cells and that the administration of Zoledronic acid, a well-known anti-resorptive agent, is effective in reducing tumor burden but only in osteoporotic animals, suggesting the existence of mechanism related to the metabolic state of bone. *[Ottewell et al, 2011]*

Starting from these evidence, the deepening of the mechanisms underlying the link between OP and metastatic progression have brought to light an interaction which appears more and more as a mutual rather than one way.

This aspect has been well highlighted in a recent paper by Pagani et al, in which, a co-culture *in vitro* model between rat breast cancer cells and OBs isolated from healthy and osteoporotic rats was set up to study this reciprocal influence. Results showed in fact, on the one hand, that the presence of cancer cells induced an increasing in the proliferation rate, mineralization and synthesis of ALP, IL-8, RANKL/OPG ratio in osteoporotic OBs and, on the other hand, that the conditioned medium of osteoporotic OBs stimulated positively breast cancer cells migration. *[Pagani et al, 2016]*



# **AIM OF THE PROJECT**

Aim of the project was to evaluate the influence of altered bone remodeling, in particular the condition of OP, on the establishment and development of bone metastases.

To reach the goal, it was proceeded with the following steps:

- Development and characterization of *in vitro* advanced models of bone tissue culture  
(rat calvaria segments and femoral condyles cultures)
  - Characterization of rat breast cancer cell line
- In vitro co- culture of rat breast cancer cells and OCs isolated from osteoporotic rats
- Development and set up of an *in vitro* advanced tridimensional (3D) model co-culturing rat breast cancer cells with bone segment harvested from health and osteoporotic rats
- *In vivo* set up of a rat model of osteolytic bone metastases in state of OP in order to confirm *in vitro* assessment



# **CHAPTER 2-**

# **MATERIALS AND METHODS**



## 2.1 ASSESSMENT OF RAT BONE CULTURES

### 2.1.1 Calvaria and Femoral Condyles Bone Cultures- Experimental set up

Calvaria bone segments and distal femoral epiphyses were obtained at euthanasia from rats involved in uncorrelated studies, approved by the Rizzoli Orthopedic Institute Ethical Committee, not affecting the health of bone or joints (study code 430/2015-PR “*Scaffolds ceramici associati a cellule staminali mesenchimali per l’artrodesi vertebrale: studi in vitro ed in vivo per la chirurgia ‘one step’ in osso sano ed osteoporotico*”).

Rats underwent pharmacological euthanasia via injection of 0.3mL/Kg of Tanax- Hoechst. Drugs used for anesthesia and euthanasia were considered not to have effects on bone segments harvested and on the subsequent tests performed. After harvesting, calvaria bone segments were cultured in Roswell Park Memorial Institute (RPMI 1640) medium (Sigma-Aldrich, Saint Louis, Missouri, USA) implemented with Bovine Serum Albumine (BSA) (Sigma-Aldrich, Saint Louis, Missouri, USA) 2 mM glutamine and antibiotics (100 U/ml penicillin, 100 µg/ml streptomycin) (Gibco, INVITROGEN Corporation, Carlsbad, CA).

Femoral condyles were cultured in Dulbecco’s Modified Eagle’s Medium (DMEM) High glucose (Sigma, MO, USA) supplemented with 10% fetal bovine serum (FBS, Lonza, Verviers, Belgium), 2 mM glutamine and antibiotics (100 U/ml penicillin, 100 µg/ml streptomycin) (Gibco, INVITROGEN Corporation, Carlsbad, CA).

Both calvaria and femoral condyles were kept in culture at 37°C, 5% CO<sub>2</sub> up to 4 weeks, in vent cap tubes under continue oscillation. Assessment of viability and microtomographical evaluations were performed at time zero; viability was further checked weekly up to 14 days. At the end of the latest experimental time, calvaria segments and femoral condyles were collected and microtomographical and histological evaluations were repeated.

The weight of cultured femoral condyles was also checked at time zero, 24 hours and up to 2 weeks to assess whether the absence of mechanical load could alter the mass during the

culture period. The samples were weighed in sterility, placed inside a tube of known weight, with an analytical scale and weight was calculated as the difference with the tare of the tube.

### ***2.1.2 Assessment of bone cultures viability***

For both bone tissue cultures viability was evaluated through Alamar blue dye test (Serotec, Oxford, UK). Briefly, the reagent is a dye, which incorporates an oxidation-reduction (REDOX) indicator that changes color in response to the chemical reduction of growth medium, resulting from cell growth. The dye was added to each culture (1:10 v/v) for 4 h at 37°C. At the end of experimental time, the supernatants were transferred to 96 well-plates, the absorbance was read spectrophotometrically at 570 and 600 nm wavelengths (for the fully oxidized and reduced forms of reagent) by MicroPlate reader (BioRad, CA, USA). The results, obtained as optical density (OD), were processed following manufacturer's instruction and expressed as reduction percentage.

### ***2.1.3 Bone cultures microtomography***

Both femoral condyles and calvaria segments in culture were scanned at time zero and 14 days with the high-resolution microtomography (microCT) system Skyscan 1172 (Bruker Micro-CT, Belgium). The source voltage was set on 70 kV with a current of 141  $\mu$ A and an Aluminum filter 0.5 mm thick was interposed between the x-ray source and the sample. Each sample was rotated until 180° with a rotation step of 0.45°. The images obtained from acquisition were later reconstructed by the software NRecon (version 1.6.10) with corrections for alignment, depended on acquisition, beam hardening and ring artifact reduction. Calvaria images resulted jpg images had 2000x2000 pixels with a pixel size of 7.45  $\mu$ m. Femoral condyles images resulted jpg images had 4000x4000 pixels with a pixel size of 4.96  $\mu$ m.

#### ***2.1.4 Bone cultures histology***

Femoral condyles and calvaria segments were harvested at the end of experimental time and processed for paraffin embedding. More in details, femoral condyles and calvaria segments samples were fixed in 10% neutral buffered formalin (Sigma-Aldrich, Saint Louis, Missouri, USA) for at least 24 hours at room temperature. After rinsing in running tap water, samples were decalcified in 5% solution of formic (ACEF, Fiumicino, Rome, Italy) and nitric acid (Sigma-Aldrich, Saint Louis, Missouri, USA) at 37°C and then extensively rinsed in distilled water. Each condyle was cut along the major axis to help the inclusion, and all samples dehydrated in increasing ethanol solutions (Panreac AppliChem, Barcelona, Spain) for 1 hours each (70%, 95% twice, 100% twice), to remove the aqueous component and facilitate the penetration of the embedding medium, and defatted in xylene (VWR International, Milan, Italy). After overnight infiltration in liquid wax (56°C), samples were finally embedded in paraffin (Sigma-Aldrich, Saint Louis, Missouri, USA). From tissue blocks, thin histological section (5 µm thick) were obtained by a semi-automated microtome (MicromH340E, Germany) and stained with Haematoxylin (Sigma-Aldrich, Saint Louis, Missouri, USA) and Eosin (Bio-Optica, Milan, Italy) (H/E).

Images of obtained sections were acquired with digital scanner at different magnification.

#### ***2.1.5 Statistical analysis***

Statistical analysis was conducted was performed using the SPSS v.12.1 software (SPSS Inc., IL, USA). Data are reported as mean  $\pm$  SD at a significance level of  $p < 0.05$ . For the evaluation of culture viability and bone mass a two way ANOVA test with Holm Sidak multiple comparison test was performed, in order to assess eventual differences between groups and experimental times.

## **2.2 CHARACTERIZATION OF RAT BREAST CANCER CELL LINE (MRMT-1)**

### ***2.2.1 MRMT-1 cells proliferation and viability***

Rat breast carcinoma cells line MRMT-1 were purchased from Cell Resource Center for Biomedical Research Institute of Development, Aging and Cancer (Tohoku University 4-1, Seiryō, Aoba-ku, Sendai, Japan).

Viability and proliferation of MRMT-1 cells were assessed in different culture conditions, characterized by the addition of growing concentration of FBS to the culture medium. MRMT-1 were seeded in a 24 well plate at a density of  $2 \times 10^5$  cells/well and divided in the following groups, representing the different culture conditions:

- basal medium (RPMI 1640 medium + 1% penicillin/streptomycin) + 10% FBS
- basal medium + 1% di FBS
- basal medium only

At the end of the scheduled experimental times of 24, 48 and 72 hours, cells were detached from each well with Trypsin EDTA (Sigma-Aldrich, Saint Louis, Missouri, USA), centrifuged at 1600 rpm, resuspended in an appropriate volume of serum free medium and counted in Burker counting cells chamber using Trypan Blue 1% dye (Sigma-Aldrich, Saint Louis, Missouri, USA), able to color selectively dead cells.

### ***2.2.2 Wound healing assay***

The *in vitro* scratch wound experiments were performed according to previous studies. Briefly, control and treated cells were seeded in 6-well plates (four replicates of each sample) with 3 ml complete medium and allow to reach confluence. A reproducible scratch in the monolayer was longitudinally made the following day using sterile micropipette tips. The

process of wound closure was monitored at different time points (0, 6, 21, 30, 45 hrs) by photographing the central field of the scratches under an inverted light microscopy (Olympus CKX41, Olympus Corp, Tokyo, Japan) mounted with a digital camera (C-7070 Wide Zoom, Olympus) at 10× magnification. The pictured field was standardized each time against a horizontal line drawn on the base of the plate passing through the center of each well. Morphometric analysis of cell migration was performed by one experienced investigator blinded to the specific experimental conditions using a computerized image analysis system (Qwin, Leica Microsystem Imaging Solution, Ltd). A region of  $2.58 \times 10^6 \mu\text{m}^2$  that included the artificial scratch and the adjacent cell monolayer was selected as the standard region of interest. The wound healing effect was calculated as  $(1-A_x/A_0) \%$ , where  $A_0$  and  $A_x$  represented the empty scratch area at 0 and x hours, respectively.

### ***2.2.3 Assessment of activated pathway***

#### ***2.2.3.1 Protein quantification***

MRMT-1 cells were collected thorough centrifugation at 1500 rpm for 5 minutes at 4°C. and resuspended in Gold Lysis Buffer (GLB). Lysates were incubated in constant shaking (750 rpm) for at least 1 hour at 4°C and then centrifugated at 13200 rpm at 4°C to remove debris; finally, supernatants with proteic lysate were collected.

Cells ( $5-10 \times 10^6$ ) were centrifuged and resuspended in cold ipotonic lysis solution of five times higher volume, kept in ice for 10 minutes and then centrifuged at 1500 rpm for 5 minutes at 4°C. Pelles were resuspended again in cold ipotonic lysis solution of two times higher volume, passed 25-30 times through a syringe with needle of 25  $\mu\text{m}$  and observed at light microscope to assess the lysis.

The lysate was then subjected to a series of centrifugations to separate proteins in the three cells portions, nucleus, heavy membranes and cytosol:

Supernatant containing cytosolic fraction was additioned with PPI inhibitors, Aprotinin, Leupeptin, Na<sub>3</sub>VO<sub>4</sub> and PMSF, while pellet with heavy membrane proteic fraction was lysed in GLB+. All of the fractions were the kept in agitation (750 rpm) for one hour and then the nuclear and heavy membrane fractions were centrifuged at 14000 rcf for 10 minute at 4°C to remove cell particulates.

Quantification of the proteic contents of the samples was evaluated trough the colorimetric Lowry Method (Kit DC Protein Assay, Bio-Rad, Hercules, CA, USA). Briefly, 1 µl of sample was diluted in distilled water (1:20) and additioned with the various reagents of the kit. Samples were incubated at dark and in costant shaking for 15-30 minutes and read spectrophotometrically at 655 nm. For each protein lysate, 50 µg of protein were loaded on the gel. Sample were prepared for loading bringing them all to the same final volume by addition of GLB + and adding to each 5X Protein Sample Buffer. The samples were then boiled for 5 minutes, briefly centrifuged and then subjected to analysis by Western blotting.

### ***2.2.3.2 Western Blotting***

The protein lysates were subjected to electrophoresis on polyacrylamide gel in sodium dodecyl sulphate (SDS-PAGE) to obtain the separation of proteins according to their size. The sodium dodecyl sulphate (SDS) (CH<sub>3</sub>- (CH<sub>2</sub>)<sub>10</sub>-CH<sub>2</sub>OSO<sub>3</sub><sup>-</sup>Na<sup>+</sup>) is an anionic detergent able to strongly bind and denature proteins, with a SDS molecule binding every two amino acid residues. In this way, the original charge of the protein is completely deleted and the polypeptide is covered with negative charges in proportional numbers to amino acids that

constitute it. All gels used were made of acrylamide 10%, except for the one for immunoprecipitation made of 12% and prepared as follow:

Proteins separation was performed in vertical electrophoresis cassettes (Amersham Biosciences UK Limited, Bucks, UK), applying a constant voltage of 100 V and 1X SDS-PAGE Running Buffer made of 1% SDS, 25 mM Tris, 200 mM glycine and distilled water.

At the end of electrophoretic run, proteins were transferred through electroblotting technique to a nitrocellulose membrane Hybond-ECL (Amersham), using a Semi-dry Transblotter (Sigma-Aldrich Corporation) and 1X Transblotting Buffer, under the constant amperage of 400 mAmps for almost two hours. The transfer of the proteins to the membrane was proven by Ponceau S staining, which bind proteins nonspecifically.

Membranes were decolored with 1X PBS containing 0.05% Tween-20 (PBS/T) and incubated at 4°C overnight in saturation buffer with 5% non-fat dry milk in PBS/T. Blots were washed three times in PBS/T and incubated overnight at 4°C with the primary antibody diluted in 5% BSA in PBS/T and specifically:  $\alpha$ -p-AKT T308 (1:1000),  $\alpha$ -p-AKT S473 (1:1000),  $\alpha$ -AKT (1:1000),  $\alpha$ -p-PKR T451 (1:1000),  $\alpha$ -p-eIF2 $\alpha$  S51 (1:1000),  $\alpha$ -p-GSK-3 $\alpha$ / $\beta$  S21/9 (1:1000),  $\alpha$ -GSK-3 $\beta$  (1:1000) and  $\alpha$ - $\beta$ -actin (Cell Signaling Laboratories, Danvers, MA, USA);  $\alpha$ -PKR (D-20) (1:1000) and  $\alpha$ -eIF2 $\alpha$  (FL-315) (1:1000) (Santa Cruz Biotechnology, La Jolla, CA, USA);  $\alpha$ - $\beta$ -Tubulin I (1:5000) (Sigma-Aldrich Corporation, Saint Louis, MO, USA);  $\alpha$ -Lamin B (1:1000) (Oncogene Research).

At the end of incubation, membranes were washed three times with PBS/T and incubated for two hours with secondary antibody conjugated with horseradish peroxidase (HRP) (Cell Signaling Technology, Inc) diluted 1:2000 in 5% of non- fat dry milk in PBS/T. For each primary antibody, one of the two secondary antibody  $\alpha$ -rabbit:HRP or  $\alpha$ -mouse:HRP was used:  $\alpha$ -rabbit:HRP:  $\alpha$ -p-AKT T308 e S473,  $\alpha$ -AKT,  $\alpha$ -p-PKR T451,  $\alpha$ -PKR (D-20),  $\alpha$ -p-

eIF2 $\alpha$  S51,  $\alpha$ -eIF2 $\alpha$ ,  $\alpha$ -p-GSK-3 $\alpha$ / $\beta$  S21/9,  $\alpha$ -GSK-3 $\beta$  and  $\alpha$ - $\beta$ -actina;  $\alpha$ -mouse:HRP:  $\alpha$ - $\beta$ -Tubulina I and  $\alpha$ -Lamin B.

Blots were washed three times in PBS/T and visualized through ECL (Enhanced ChemiLuminescence) Western blotting reagent (Amersham, Rockford, IL, USA). It is a method for detection of antigens, directly or indirectly conjugated with an antibody labeled with HRP, which uses the non radioactive light emission. In alkaline conditions, peroxidase catalyzes luminol oxidation which get an excited state; during the decay to the basal condition, luminol releases the excess energy by emitting light that can impress a photographic plate. The ECL Western blotting method uses, also, the presence of chemical enhancers of oxidation (such as phenols), enhancing in this way both the duration and the intensity of light emission. The bands corresponding to the various proteins of interest were exposed on photographic plates (Kodak) and their intensity was estimated by densitometric analysis using the software Image J. Briefly, plates were scanned and saved as JPEG files 8-bit greyscale. The percentage of pixels measurable in the images has been set using the adjustment control of the image background and then the number of pixels was estimated in the selected area, corresponding to the band of the protein.

Immunoprecipitation assay exploits the interaction antibody- antigen to precipitate specific antigen present in a solution (for example, cellular lysate). Once added the antibody to the solution, it will recognize and bind its antigen forming soluble antigen-antibody complex. In order to isolate such complexes, an immunoglobulin binding protein, such as protein A or G, was used, associated covalently to an insoluble support, such as agarose, that allows to precipitate by centrifugation, via increasing the molecular weight of the complex. The immunoprecipitation was conducted on CEM cells in logarithmic growth phase. Following extraction of total protein and the determination of protein concentration, two sample volumes corresponding to 500 micrograms of proteins were transferred to 1.5 ml tubes to be



subjected to immunoprecipitation , while 100 micrograms of proteins were transferred to a third tube to be used as a control.

At each of the two samples were added 25  $\mu$ l of Protein A /G PLUS-Agarose Immunoprecipitation Reagent (Santa Cruz Biotechnology, Inc.) and 200  $\mu$ L of the GLB + and all was placed in cold room and in rotation for two hours. This phase had the aim of immunoprecipitate cellular proteins capable of forming non-specific bonds with the protein A /G. After incubation, the samples were centrifuged at 13,200 rpm at 4 °C for 1 min and the supernatants were transferred to two new tubes to which are added:

- Sample 1: 5  $\mu$ l antibody  $\alpha$ -p-Tyrosine mouse mAb (Cell Signaling Technology) and 25  $\mu$ l of Protein a / G PLUS-agarose
- Sample 2: 5  $\mu$ l antibody  $\alpha$ -PKR (D-20) (Santa Cruz Biotechnology, Inc.) and 25  $\mu$ l of Protein a / G PLUS-agarose. Both samples were incubated overnight at 4°C in rotation.

The next day, the antigen-antibody complexes were precipitated by centrifugation at 13200 rpm for 1 minute to 4°C. The pellets so obtained underwent 4 washes with 500  $\mu$ L of GLB + after which each pellet was resuspended in 20  $\mu$ l of GLB + and additioned with 5X protein sample buffer. Samples undergone to immunoprecipitation and control samples were boiled for 5 minutes, centrifuged and analyzed by SDS-PAGE followed by immunoblotting. The blots of the control sample and of the sample with the antibody immunoprecipitated  $\alpha$ -p-Tyrosine (samples 1) were incubated with the primary antibody  $\alpha$ -PKR (D-20), while for the sample immunoprecipitated with  $\alpha$ -PKR (D- 20)  $\alpha$ -p-Tyrosine was used as primary antibody. For both the primary antibodies dilutions of 1: 1000 in 5% BSA in PBS / T were used, while the secondary  $\alpha$ -rabbit: HRP was diluted 1: 2000 in 5% skimmed milk in PBS / T.

## **2.2.2 MRMT-1 cells sensitivity to doxorubicin**

### **2.2.2.1 Experimental culture set up**

Doxorubicin is a cytotoxic anthracycline antibiotic isolated from cultures of *Streptomyces peucetius* var. *caesius*. Doxorubicin binds to nucleic acids, presumably by specific intercalation of the planar anthracycline nucleus with the DNA double helix.

The chemotherapeutic Doxorubicin (Doxorubicin 5 mg powder, Vinci-Biochem, Vinci, Italy) was resuspended in culture medium RPMI 1640 at a concentration of 100 µM. Subsequently serial dilutions of Doxorubicin were prepared to get five drug concentrations (5 µM, 2.5 µM, 1 µM, 0.5 µM, 0.1 µM)

MRMT-1 cells were seeded in a 96 well plate at a density of  $2 \times 10^4$  cells/well in standard culture medium. 24 hours after seeding, culture medium was refed as described below:

- RPMI 1640 medium + 1% penicillin/streptomycin (basal medium) + 10% FBS
- basal medium + 1% FBS
- basal medium without FBS

and to each group the different doxorubicin concentrations previously prepared were administered. As controls, for each group cells cultured with the same medium but not exposed to the drug were used. At the end of the expected experimental time, cell viability was assessed through WST-1 assay.

### **2.2.2.3 Evaluation of cells viability**

Briefly, the WST-1 assay is a colorimetric test to assess cell viability via the mitochondrial respiration. The salt of stable tetrazolium WST-1 is cleaved into soluble formazan by a complex cellular mechanism that takes place primarily at the cell surface. This reaction of

bioriduction depends strictly on the glycolitic production of NAD(P)H in viable cells. Therefore, the increase of the formed formazan dye directly correlates with the number of metabolically active cells present in culture.

The cells were washed with PBS 1%, and thereafter WST-1 was added in a concentration of 1:10 to the culture media. The plates were incubated for 4h at 37 ° C, 5% CO<sub>2</sub>; at the end of the incubation time, the formed dye is quantified spectrophotometrically at an absorbance of 450 nm.

The IC<sub>50</sub>, namely the concentration of the drug able to inhibit 50% of cell survival compared to controls, was determined by comparing cell viability and the logarithmic concentration of doxorubicin used in a dose response semi-log curve.

### ***2.2.3 Statistical analysis***

Statistical analysis was conducted on the viability test for Doxorubicin sensitivity to assess differences in the effects of drug concentration. The analysis was performed using the SPSS v.12.1 software (SPSS Inc., IL, USA). Data are reported as mean ± SD at a significance level of  $p < 0.05$ . Differences between groups were analyzed using the Kruskal-Wallis test for independent samples.

## 2.3 CO-CULTURE OF MRMT-1 CELL LINE AND OSTEOCLASTS

**Published paper** (*Salamanna F, Pagani S, Maglio M, Borsari V, Giavaresi G, Martelli AM, Buontempo F, Fini M. Estrogen-deficient osteoporosis enhances the recruitment and activity of osteoclasts by breast cancer cells. Histol Histopathol. 2016 Jan;31(1):83-93. doi: 10.14670/HH-11-651. Epub 2015 Aug 7.*)

### 2.3.1 Conditioned media preparation

Cells were kept in culture in RPMI 1640 medium (Sigma, MO, USA) supplemented with 10% FBS (FBS, Lonza, Verviers, Belgium), 2 mM glutamine and antibiotics (100 U/ml penicillin, 100 µg/ml streptomycin) (Gibco, INVITROGEN Corporation, Carlsbad, CA) at 37°C 5% CO<sub>2</sub>. Once at confluence, cell cultures were rinsed and culture medium was substituted with serum-free RPMI 1640 to obtain conditioned medium (15 ml per T75 flask, ~ 1 x 10<sup>6</sup> cells/cm<sup>2</sup>). After twenty-four hours, medium was collected, centrifuged and stored at -80°C.

### 2.3.2 Isolation of mononuclear cells and differentiation into OCs

PBMCs were isolated from six healthy (SHAM) and six ovariectomized (OVX) Sprague-Dawley adult female rats (Charles River Calco Lecco, Italy) from an uncorrelated study approved by the Rizzoli Orthopedic Institute Ethical Committee to isolate OCs. The establishment of estrogen-deficient osteoporotic condition in OVX animals and the healthy condition in SHAM animals was assessed through quantitative bone ultrasound evaluations, microtomography and histomorphometric analysis of the iliac crest biopsy.

PBMCs were isolated onto Ficoll-Histopaque gradient (Sigma-Aldrich, MO, USA), according to the following protocol. Harvested peripheral blood was diluted 1:1 with PBS and slowly layered on Histopaque 1077 (ratio 2:1). After centrifugation at 700g for 30 min at room temperature, the mononuclear cells fraction was isolated; PBMCs were collected and,

after washing twice with PBS, resuspended in appropriate volume of basal medium - Dulbecco's Modified Eagle's Medium (DMEM, Sigma-Aldrich, MO, USA) + 10% fetal calf serum (FCS, Lonza, Verviers, Belgium) + 2 mM glutamine + antibiotics (100 U/ml penicillin, 100 µg/ml streptomycin) - to be counted in a Neubauer chamber after a brief incubation with Turk solution (to lyse the residual red cells).

$1.5 \times 10^6 / \text{cm}^2$  of the so obtained PBMCs from SHAM (PBMC<sub>SHAM</sub>) and OVX (PBMC<sub>OVX</sub>) rats were seeded in basal medium. After four days of culture, non-adherent cells were removed, while the adherent cells were reseeded with different media, according to the following experimental set up:

- Negative control (CTR-): basal medium only;
- Positive control (CTR+): differentiation medium, composed of basal medium supplemented with differentiating factors towards the OC phenotype (30 ng/ml of RANKL, 25 ng/ml of M-CSF and  $10^{-7}$  M PTH) (Peprotech, Rocky Hill, NJ);
- Basal conditioned medium (CM-): 50% basal medium + 50% conditioned medium derived from MRMT-1 cells;
- Differentiation conditioned medium (CM+): 50% differentiation medium (Peprotech, Rocky Hill, NJ) + 50% conditioned medium from MRMT-1 cells.
- Co-culture system (TW) using transwell inserts (Millicell 0.4µm pore-size, 12 mm Diameter, Millipore, Ireland): MRMT-1 breast cancer cells were seeded in the upper inserts at a density of  $1 \times 10^3$  cells in 500 µl of RPMI 1640, while  $1.5 \times 10^6$  PBMC<sub>SHAM</sub> or PBMC<sub>OVX</sub> were seeded in the lower chambers in 1 ml of basal medium only.

As control of the culture groups and in order to reproduce the experimental condition, MRMT-1 cells were cultured alone in transwell inserts at a density of  $1 \times 10^3$  cells.

All cultures were kept at 37°C, 5% CO<sub>2</sub> up to two weeks; assessment were performed at one and two weeks.

Culture media were changed twice a week and then harvested, centrifuged and stored at -80°C for further assays at each experimental time.

### ***2.3.3 PBMCs viability***

Cell viability was evaluated through Alamar blue dye test (Serotec, Oxford, UK) as previously described (paragraph 2.1.2)

### ***2.3.4 OCs differentiation***

The tartrate-resistant acid phosphatase (TRAP) histochemical staining was used to assess the OC differentiation, according to manufacturer's instructions (387A-KT, Sigma-Aldrich, MO, USA). In the evaluation, large cells which showed four or more nuclei and with a brown staining were scored as positive cells. Through an image analysis system (Leica QWIN, Leica Microsystems Ltd, UK) the ratio (TRAP RGB %) between the brown colored region and total image area was measured, defining the brown color on the red-green-blue (RGB) scale as [R= 36÷86; G=23÷40; B=14÷24]. Images were captured at 40x magnification using a standard light microscope (Olympus IX71, Olympus Italia Srl, Italy) equipped with a digital camera (XCell, Olympus Italia Srl, Italy). The assessment were performed by two experienced and blinded investigators, in order to overcome any bias.

### ***2.3.5 OCs synthetic activity***

Supernatants collected from each culture condition were centrifuged to remove particulates and used for the following assays:

- total protein content (Total Protein Kit, Micro Lowry method, Petterson's Modification, Sigma-Aldrich, MO, USA)
- cathepsin K (CTSK)

- transforming growth factor-beta 1 (TGF- $\beta$ 1)
- tumor necrosis factor alpha matrix (TNF- $\alpha$ )
- vascular endothelial growth factor (VEGF)
- matrix metalloproteinase-7 (MMP-7)
- matrix metalloproteinase-9 (MMP-9) (Enzyme-linked Immunosorbent Assay Kits, Uscon Life Science Inc., Wuhan, China).

The release of CTSK, TGF- $\beta$ 1, TNF- $\alpha$ , VEGF, MMP-7 and MMP-9 by PBMC in culture was calculated as difference between supernatant total content and MRMT-1 synthesis in the different culture conditions (CM+, CM- and TW).

### ***2.3.6 Statistical analysis***

Statistical analysis was performed using the SPSS v.12.1 software (SPSS Inc., IL, USA). Data are reported as mean  $\pm$  SD at a significance level of  $p < 0.05$ . The Kolmogorov Smirnov test was performed to test normality of the variables. The General Linear Model (GLM) with adjusted Sidak's multiple comparison test with 'culture type' (CTR-, CTR+, CM+, CM-, TW) and 'cell type' (SHAM and OVX) as fixed effects was performed to assess the differences between factors on PBMC viability, OC differentiation and synthetic activity within each experimental time. In particular, the following comparisons were taken into account:

- within each 'cell type': (A) SHAM versus OVX;
- within each 'culture type': (1) CTR+ versus CTR-; (2) CM+ versus CTR+; (3) CM- and TW versus CTR-;

at first to evaluate the influence of osteoporotic condition on OC behaviour within each 'cell type' and secondly to understand if exogenous factors present in culture medium (CTR+) and the different 'culture type' might have an influence on OC response.

## 2.4 ASSESSMENT OF A 3D MODEL OF RAT BONE METASTASES *IN VITRO*

### 2.4.1 *Experimental set up*

Calvaria bone segments were obtained at euthanasia from SHAM and OVX rats involved in an uncorrelated study, approved by the Rizzoli Orthopedic Institute Ethical Committee. After harvesting, bone segments were cultured in RPMI 1640 medium (Sigma, MO, USA) implemented with BSA (Sigma, MO, USA) 2 mM glutamine and antibiotics (100 U/ml penicillin, 100 µg/ml streptomycin) (Gibco, INVITROGEN Corporation, Carlsbad, CA) and divided in four groups according to the following experimental set up:

- **SHAM/OVX:** SHAM/OVX calvaria bones cultured alone
- **SHAM/OVX + MRMT-1:** SHAM/OVX calvaria bones co- cultured with rat breast cancer cells MRMT-1

24 hours after harvesting, all calvaria segments were placed in co- culture with MRMT-1 cells, seeded at a density of  $2.5 \times 10^5/\text{mL}$  in a final volume of 3 mL of culture medium for each sample. Cultures were kept in a TubeSpin Bioreactor in constant shaking (20° inclined plan, 5 revolution per minute) up to two weeks at 37°C, 5% CO<sub>2</sub>. (**Figure 2.1**) Viability of bone segments was checked at time zero, one and two weeks with Alamar Blue assay following the protocol described in the paragraph 2.1.2. Briefly, to perform the assay, bone segments were taken from the culture and tested alone; supernatants were centrifuged and stored at -80°C for further assays, while the eventual pellet found at the end of the centrifugation was tested to evaluate the presence of viable cells circulating in the culture media. At the end of the assay, bone segments were put in culture again maintaining the same original culture conditions with new culture media. At the end of the latest experimental time, bone samples were harvested for evaluation of breast cancer



cells protein expression, isolated through cold detachment with Trypsin EDTA, and paraffin histology of calvaria samples as previously described (paragraph 2.1.4)

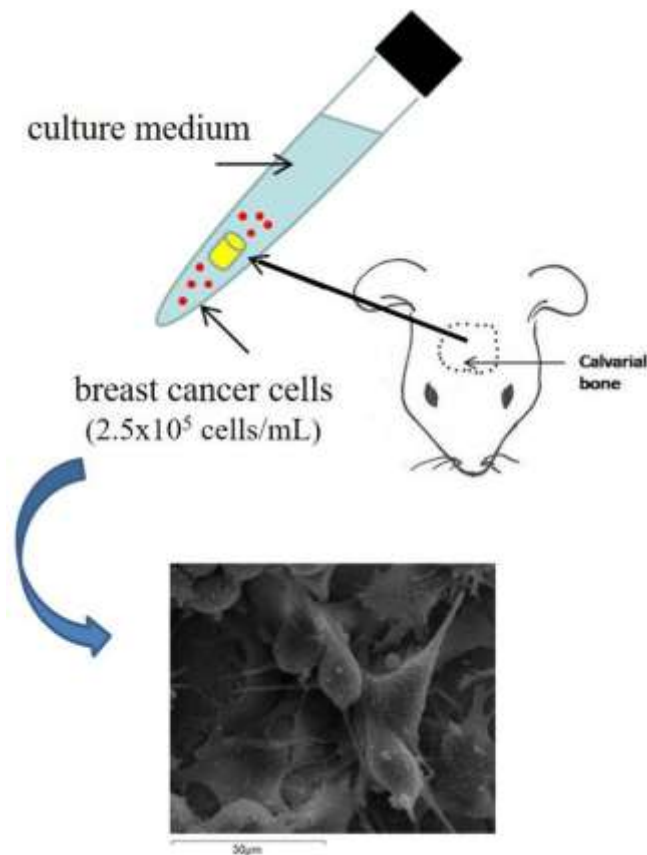


*Figure 2.: Experimental set up of 3D culture of calvaria segments and MRMT-1 cells.*

### **2.1.8 Statistical analysis**

Statistical analysis was conducted was performed using the SPSS v.12.1 software (SPSS Inc., IL, USA). Data are reported as mean  $\pm$  SD at a significance level of  $p < 0.05$ . For the evaluation of culture viability univariate ANOVA test with Gabriel post hoc test was performed, having the size of the subgroups not equal, in order to assess eventual differences between groups and experimental times.

## 2.5 *IN VIVO* INDUCTION OF OSTEOLYTIC LESION

The *in vivo* experimental protocol was presented and approved by Ethics Committee of Rizzoli Orthopaedic Institute (“Ruolo del microambiente osteoporotico nello sviluppo di metastasi ossee. Studio *in vivo*”) and by the Italian Health Ministry. The study was conducted in compliance with Italian and European laws on animal experimentation (Legislative decree of January 27, 1992, No. 116) and the animals were housed in standard conditions according to Italian Law 116/92, and the Commission Recommendation of the European Communities of 18 June 2007 on guidelines for the accommodation and the care of animals used for experimental and other scientific purposes.

For the study, twenty-eight Fisher inbred female rats, weight  $228 \pm 20$  grams, (Charles River, Calco, Lecco, Italy) were used. Before starting the study, rats were divided in two groups as follows:

- 16 rats underwent bilateral ovariectomy to induce an osteoporotic condition, going to be the “Osteoporotic” OVX group;
- 12 rats underwent a surgery only simulating the ovariectomy by removing and returning ovaries intact to their original position, going to be the “healthy” SHAM group.

The animals were housed in individual cages in standard conditions ( $22 \pm 1$  °C and  $55 \pm 10$  % UR, with ventilation of 10 air/ changes per hour) and were fed with a standard maintenance diet (Laboratori Piccioni srl, Gessate, Milan, Italy) and water at libitum.

### 2.5.1 *Surgical procedure*

After 16 weeks from ovariectomy, animals were subjected to surgical procedure for induction of osteolytic lesion. [*Fini et al, 2013*] After 10 days of quarantine, general anaesthesia was induced with an intramuscular injection of Ketamine 87 mg/kg (Imalgene 1000, Merial Italia S.p.A, Milan, Italy) and Xylazine 3 mg/kg (Rompun, Bayer S.p.A., Milan, Italy). Under

sterile conditions, the medial region of right proximal tibial metaphysis was surgically exposed; then, using a 23-gauge needle immediately below the growth plate, the tibia was pierced. The needle was then removed and replaced with a thin blunt needle (Hamilton needle, Hamilton Company, Bonaduz, GR, CH) attached to a 5  $\mu$ l Hamilton syringe (Hamilton Syringe, Bonaduz, GR, CH).  $3 \times 10^3$  MTMT-1 cells resuspended in 3  $\mu$ l of RPMI 1640 culture medium were so injected in the tibia. **(Figure 2.2)**



*Figure 2.2: Injection of MRMT-1 cells in rat tibia trough Hamilton syringe*

After the injection, the needle was removed to allow the distribution of cells, preventing spillage or excessive bleeding by using bone wax to fill the hole.

### ***2.5.2 Imaging evaluation of lesions development with Positron Emission Tomography (PET)***

At the scheduled experimental time of 7 and 14 days, all rats underwent imaging investigation through the use of a microPET to assess the development of the lesions. Rats were kept under fasting condition and water ad libitum from the day before the test. Before starting the procedure, rats were weighted and serum glucose levels were tested.  $^{18}\text{F}$ -FDG was injected through the tail vein and rats maintained under the same light condition for 40' before being positioned on the bed and starting the scanning. At the end the last experimental time, animals underwent pharmacological euthanasia by intravenous administration of 0.5 ml Tanax (Intervet Italia S.r.l., Segrate, Milan, Italy) and the entire tibiae were harvested for histological evaluation.



# **CHAPTER 3-**

# **RESULTS**

### 3.1 ASSESSMENT OF RAT BONE CULTURES

**Calvaria bone culture**- Evaluations on calvaria bone segments showed that viability of samples remained stable during the 14 days of culture, with values comparable to those of time zero. No significant differences were found between the experimental times. **(Figure 3.1)**

Microtomographical and histological assessment of samples did not highlight any alterations in the morphology and microarchitecture of the cultured calvaria bones. It could be appreciable the extensive presence of osteocytes entrapped in the mineralized bone, filling the lacunae. In some cases, part of the cranial sutures are detectable, with the presence of dense fibrillar connective tissue. **(Figure 3.2)**

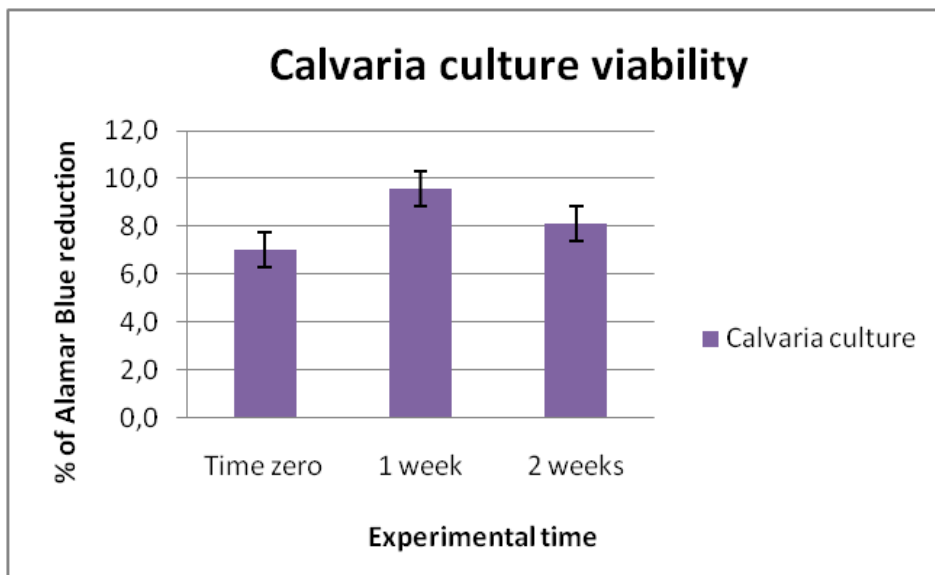


*Figure. 3.1: Viability trend of calvaria bone cultured up to 14 days evaluated through Alamar Blue assay.*

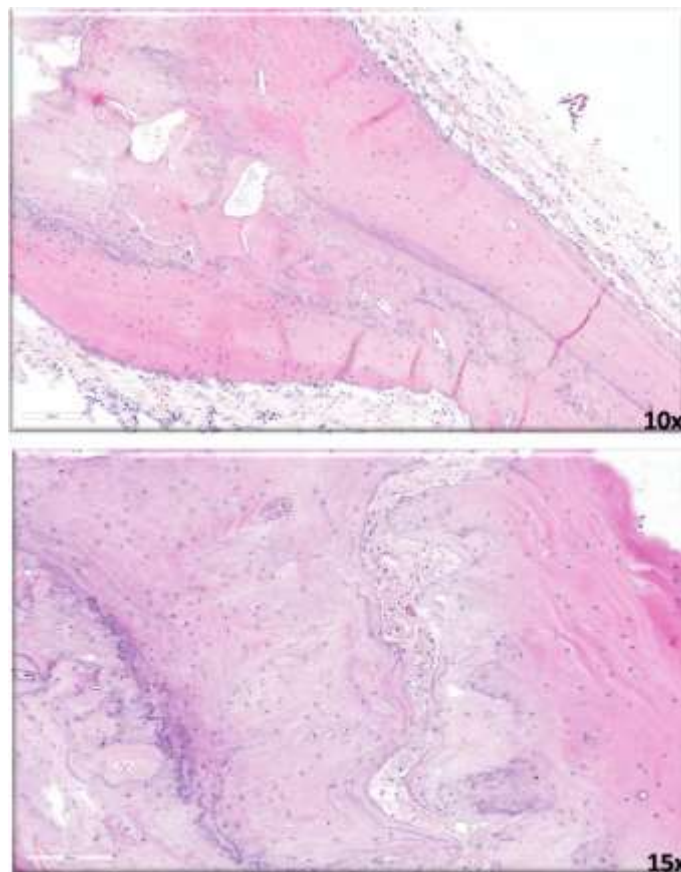


*Figure. 3.2: 3D reconstructions by microCT and histological images of calvaria bone segments after in vitro culture. Hematoxylin/Eosin staining.*



**Femoral condyles culture-** Data obtained from cultures of femoral condyles at each experimental times indicated that the culture system was able to maintain both the viability and the mass of the bone segments up to 14 days. Viability of femoral condyles remained almost stable over time without significant differences between the experimental times evaluated. By the way, between the first and the second week of culture, it could be observed a positive trend in terms of viability, whose values remained almost unchanged up to the latest experimental time (**Figure 3.3**). No differences in bone mass were detected between the beginning and the end of the experiments. (**Figure 3.4**)

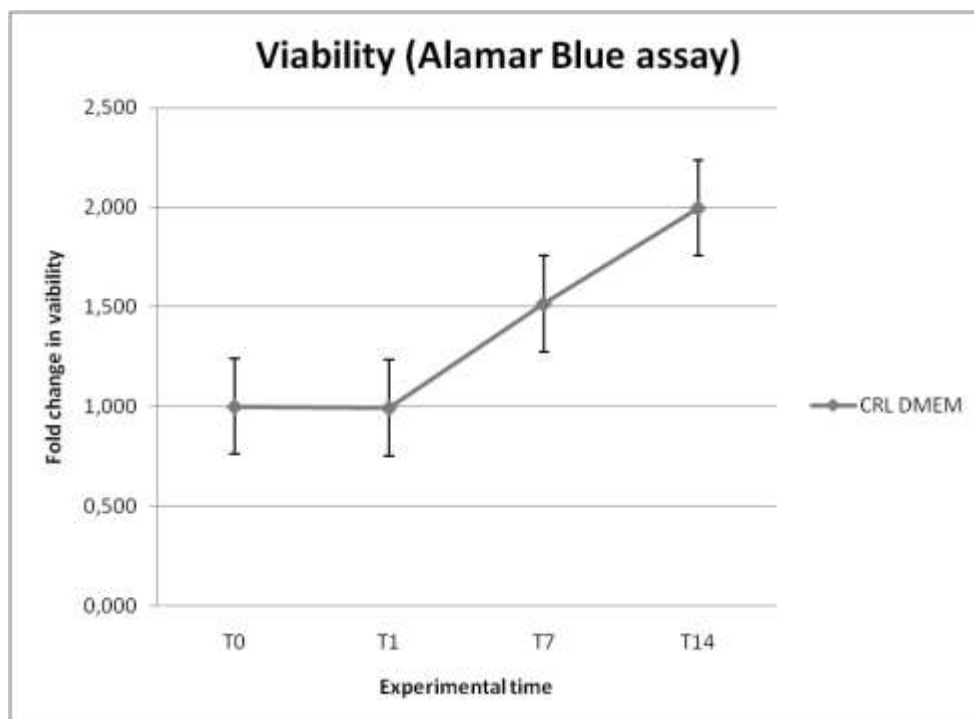


*Figure. 3.3: Viability trend of femoral condyle bone cultured up to 14 days evaluated through Alamar Blue assay.*

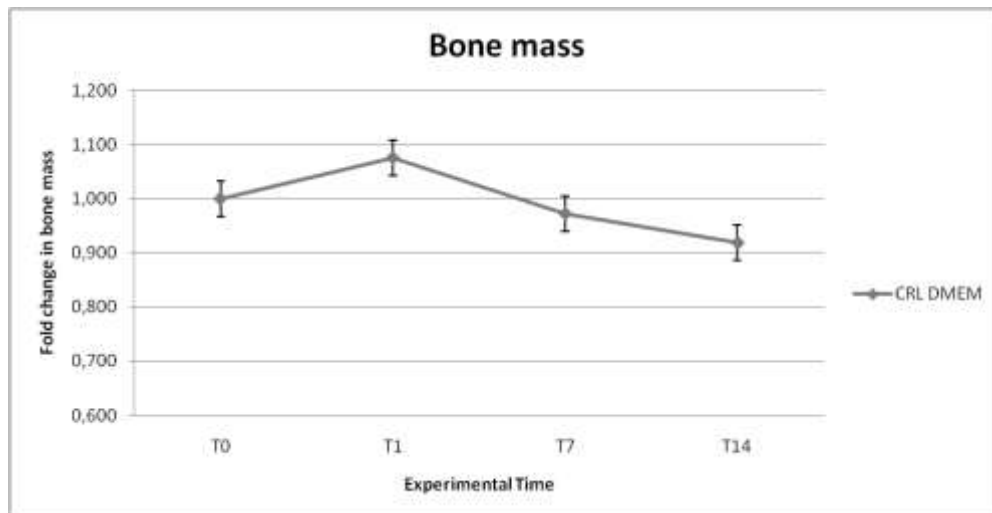


*Figure 3.4.: Fold change in femoral condyle mass during in vitro culture.*

Microtomographical assessment revealed no differences in bone structure throughout the course of the culture. Histological observation highlight no alteration in bone structure, which seemed to preserve its native appearance, with lacunae filled with osteocytes and absence of signs of necrosis or sufferance. Only a few depletion of bone marrow component could be observed for samples harvested at 14 days in comparison to bone at time zero; this occurrence, however, can be attributed to the long term of the culture (**Figure 3.5**)

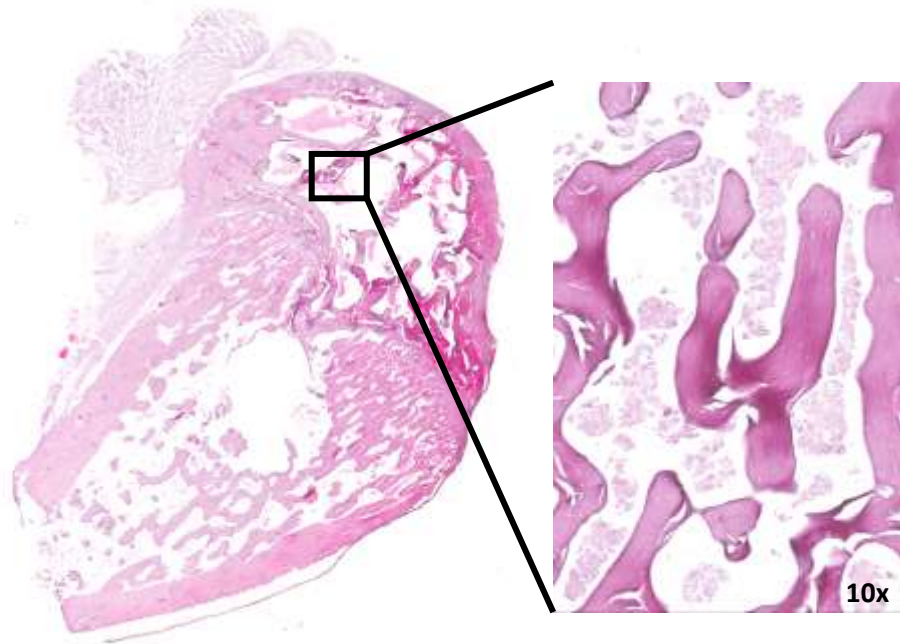


*Figure 3.5: Histological image of femoral condyle after 14 days of culture. In detail, bone trabeculae and bone marrow. Hematoxylin/Eosin staining.*

### 3.2 CHARACTERIZATION OF MRMT-1 CELL LINE

**Viability**- Values obtained at the end of each experimental times on the number of cells showed that in standard culture condition (basal medium + 10% FBS), MRMT-1 growth resulted exponential, with increasing values that are about three times those of the previous step. **(Figure 3.6)**

In the other culture conditions, cells proliferation rate decreased proportionally to the reduction of FBS percentage in the culture medium, nevertheless cell viability remained stable up to the condition without FBS addition, in which it could be observed a progressive reduction of viability of seeded cells during the experimental times. **(Figure 3.7)**

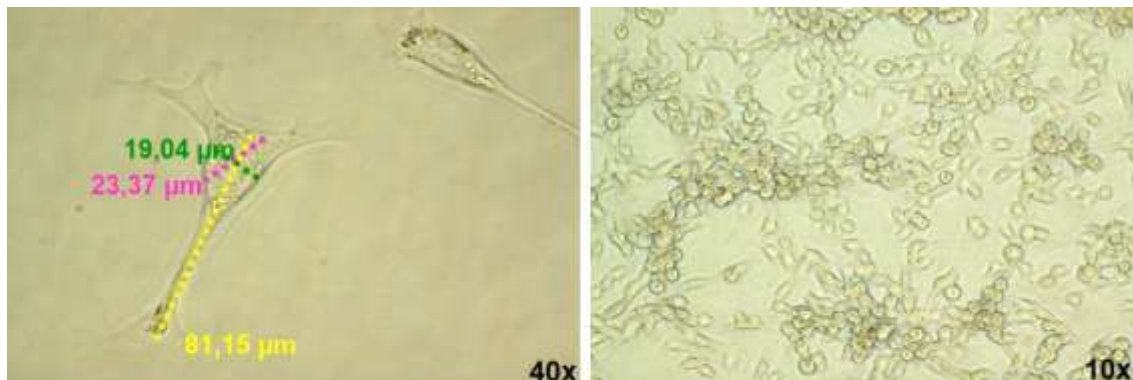


*Figure 3.6: Microscope images of MRMT-1 cells in culture.*

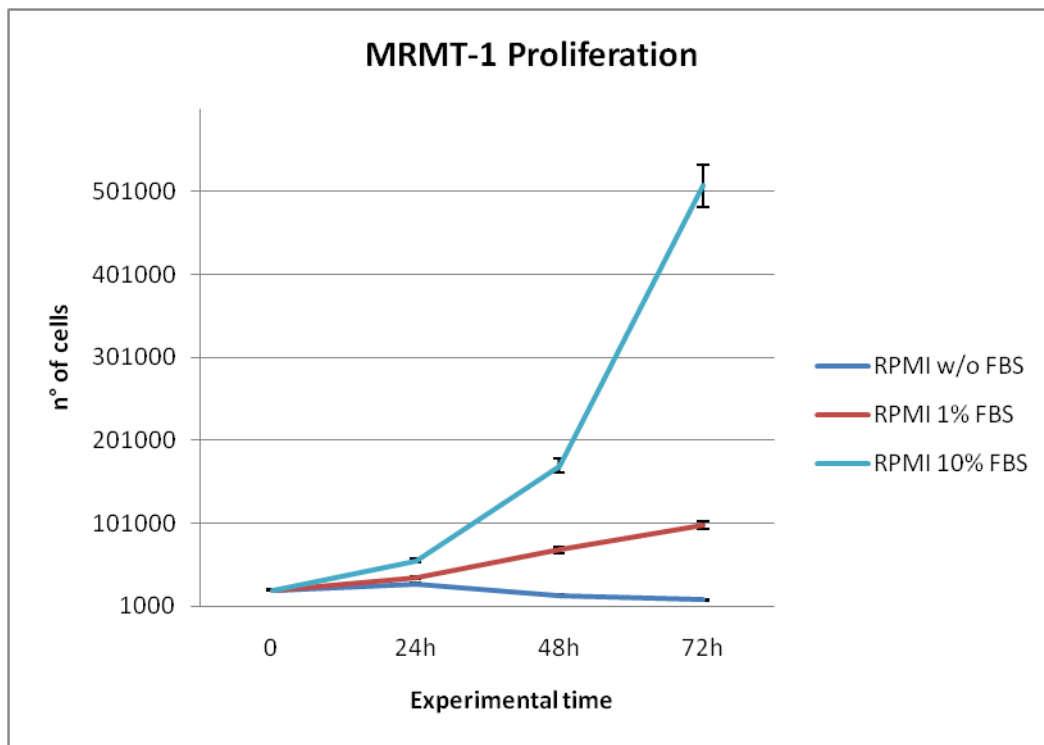


Figure 3.7: MRMT-1 trend proliferation in different culture conditions.

**Wound healing assay-** The observation up to 24 hours of MRMT-1 cells behavior showed that, already after six hours from performing the wound, cells start to migrate. The speed of migration resulted to be exponential and at 24 hours cells resulted to have heal the 80% of the wound. Applying a linear regression with the least squares method to the results obtained at the various time points evaluated (6, 12 and 24 hours) it has been estimated that MRMT-1 cells require 15 hours to heal the 50% of the wound created. **(Figure 3.8)**

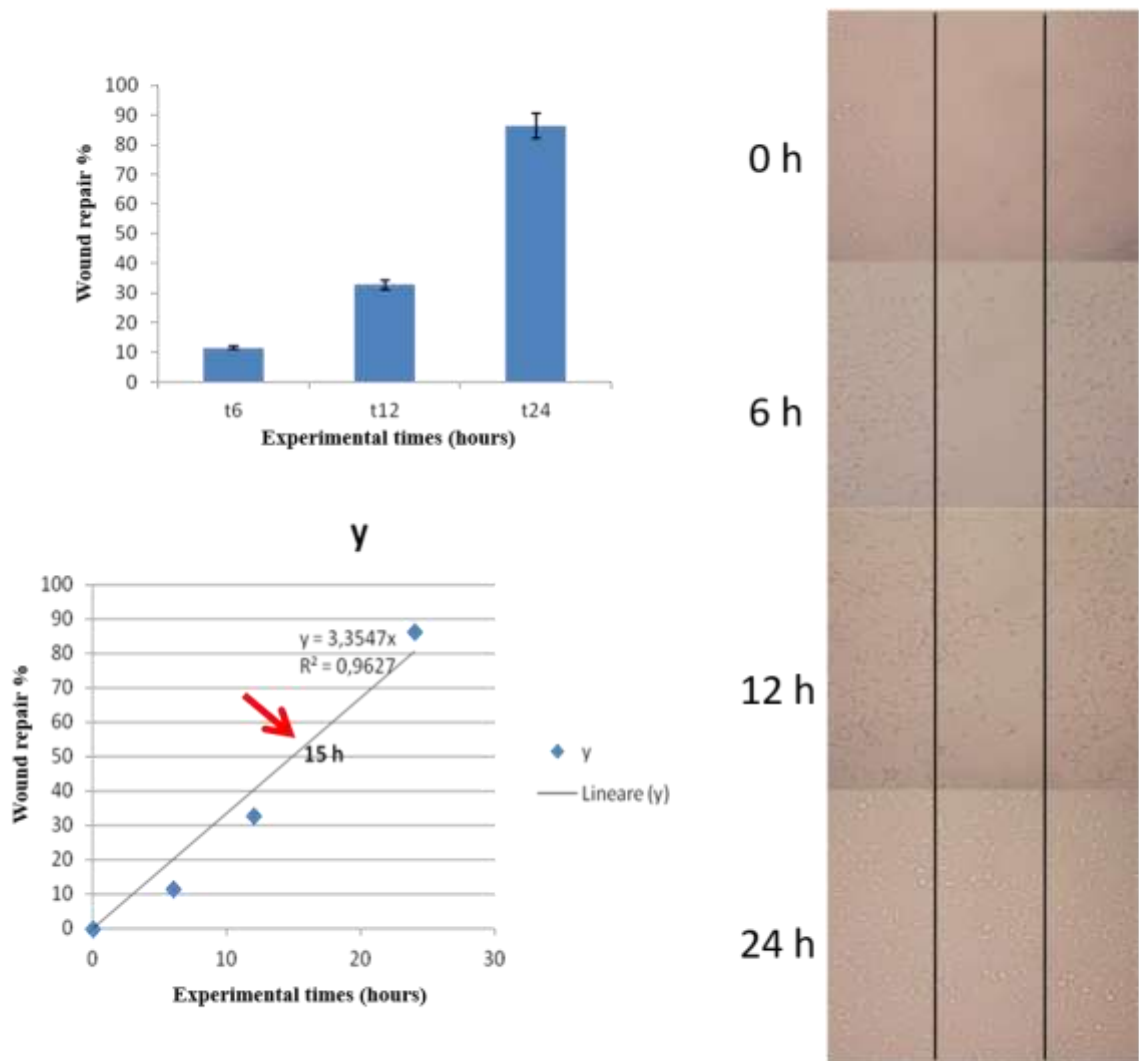


Figure 3.8: Results of wound healing assay: histograms graph of percentage of wound healing recovery, linear regression for assessing timing of 50% of recovery and microscope images of wound healing progression.

**Molecular pathways profile-** The panel obtained by the western blot assay performed on MRMT-1 cells lysate showed that the pathway of PI3K/Akt/mTOR was clearly active, and mTOR targets also appeared activated. Even the MAP kinase pathway resulted to be active, while this not can be said for the IKK/NkB and JAK kinase pathways. As expected, being a cancer cell line, p53 resulted to be phosphorylated and consequently not active. The

phosphorylation of the Protein Kinase C Delta suggested the presence and activity of CK2. MRMT-1 cells resulted also positive for the expression of the Epidermal Growth Factor Receptor (EGFR) and of MMP-9. (Figure 3.9)

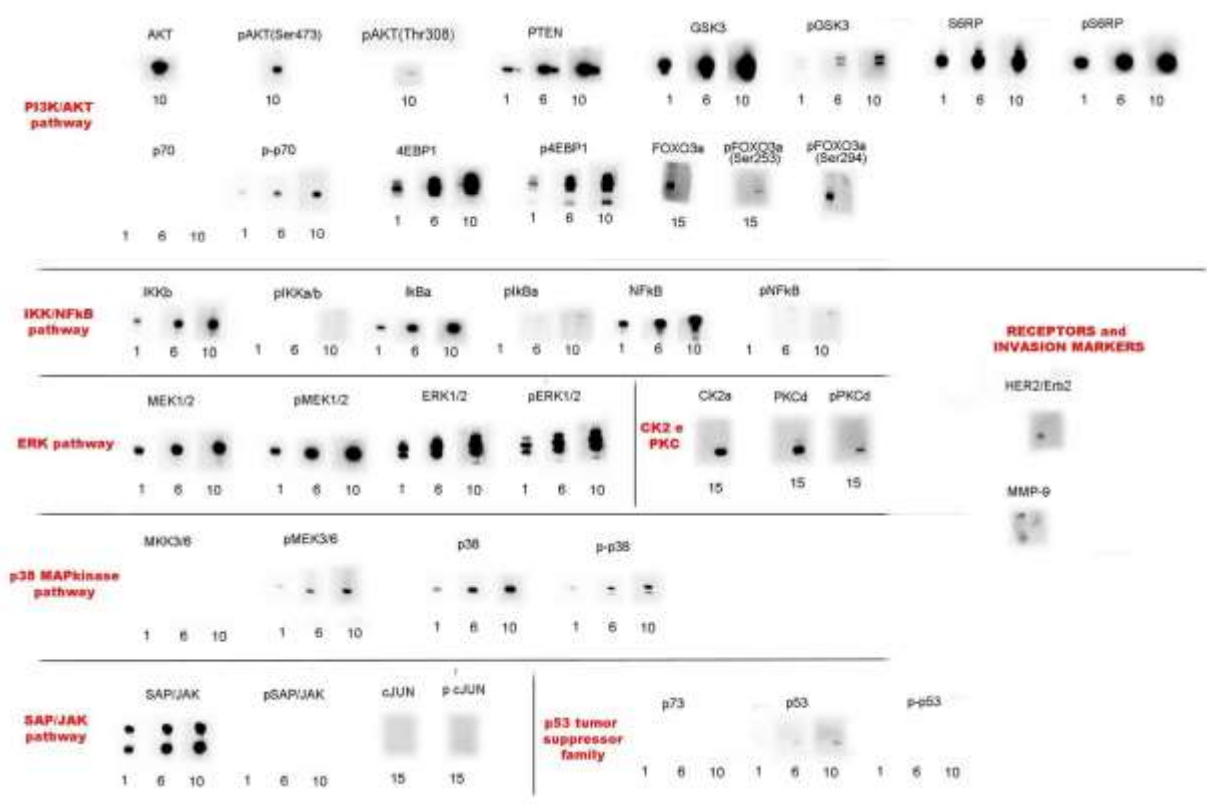
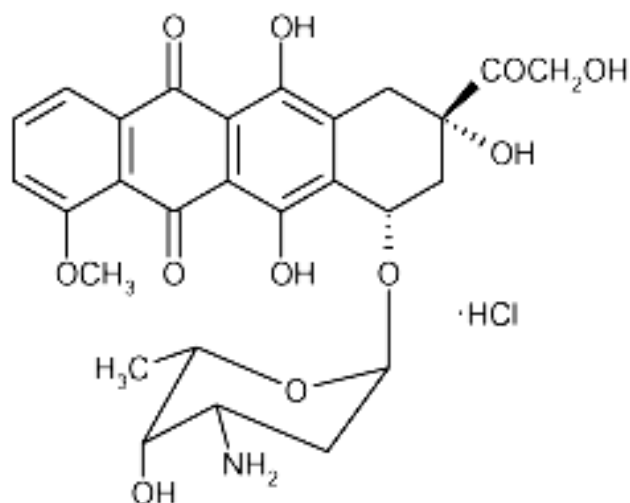


Figure 3.9: Panel of pathways activated in MRMT-1 cell line.

**Sensitivity to doxorubicin-** In standard culture condition the cytotoxic effect of doxorubicin begins to appear already at the shorter experimental times (24 – 48 hours) only in the groups exposed to higher concentrations of doxorubicin (2.5-5  $\mu$ M); at 72 hours, it could be observed a sharp drop in viability of up to 50% for cells exposed to concentrations of 2.5 and 5  $\mu$ M doxorubicin. (Figure 3.10)



*Figure 3.10: Doxorubicin chemical structure*

The results of same type of cytotoxicity test, conducted cultivating cells in media without serum and with 1% serum, showed that the viability trend of cells cultivated in medium with 1% serum and treated with doxorubicin is similar to that of the standard (10% FBS), with increased sensitivity to higher doses of the chemotherapeutic and achievement of  $IC_{50}$  after 72h of exposure to concentrations of 2.5-5  $\mu$ M. The cells cultured in serum-free medium showed instead a particular behavior, with a sensitivity to the chemotherapeutic drug almost nothing to the first two experimental times; only at 72 hours cytotoxic effect was appreciable at the highest doxorubicin concentrations. (**Figure 3.11**)

The comparison between the group highlighted significant differences for doxorubicin concentration at 2.5  $\mu$ M ( $p < 0.05$ ) and 5  $\mu$ M ( $p < 0.005$ ).



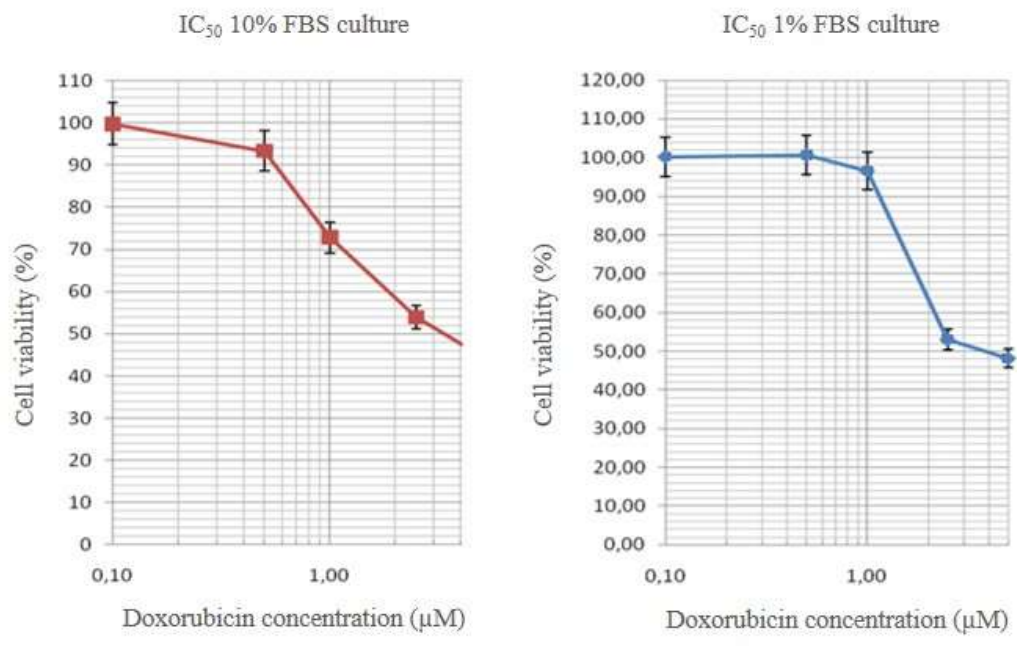


Figure 3.11: Effect of different Doxorubicin concentrations on MRMT-1 cell line

### 3.3 CO-CULTURE OF MRMT-1 CELL LINE AND OSTEOCLASTS

Data were evaluated comparing individually the osteoporotic condition with the healthy one and the different culture conditions between them, in order to highlight their influences on the trend of cultures [Salamanna et al, 2016].

The evaluation of the influence of osteoporotic condition on OCs, as regarding viability performed through Alamar Blue test, showed significant higher values where  $PBMC_{OVX}$  were present in comparison with  $PBMC_{SHAM}$  at both experimental times. (Figure 3.12)

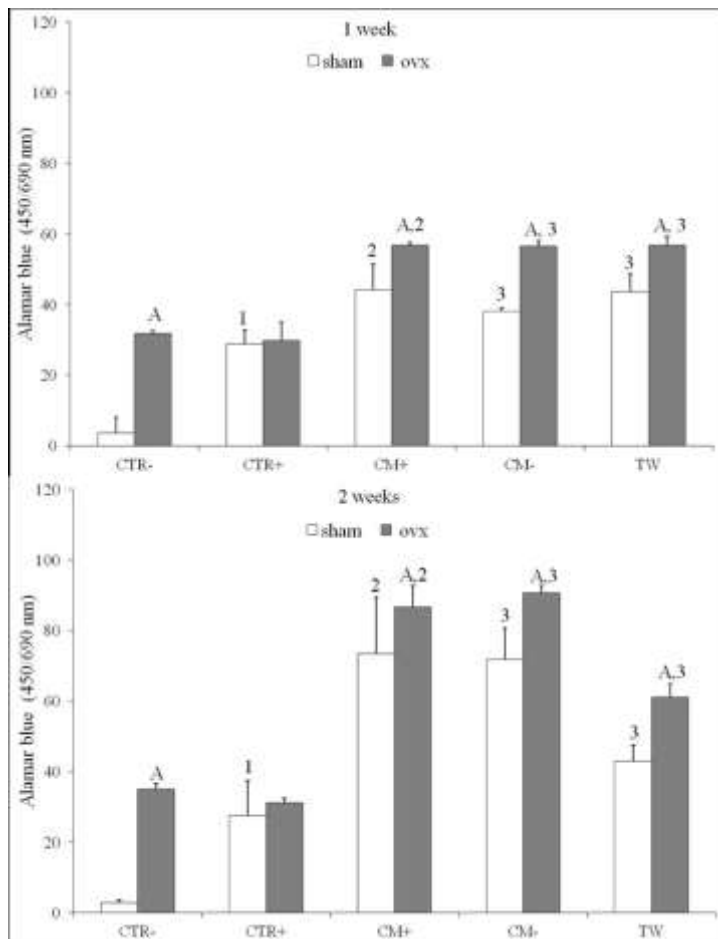


Figure 3.12: Viability trend of  $PBMC_{OVX}$  and  $PBMC_{SHAM}$  in CTR-, CTR+, CM-, CM+ and TW culture conditions at one and two weeks. [Salamanna et al, 2016]

These data are reflected also in the evaluations of TRAP staining which appeared stronger in the osteoporotic culture, in particular in CTR-, CM+ and CM- groups, already at one weeks, while at the second experimental time, the trend was maintained by CTR- and CM- cultures and expressed also by TW condition. **(Figure 3.13)**

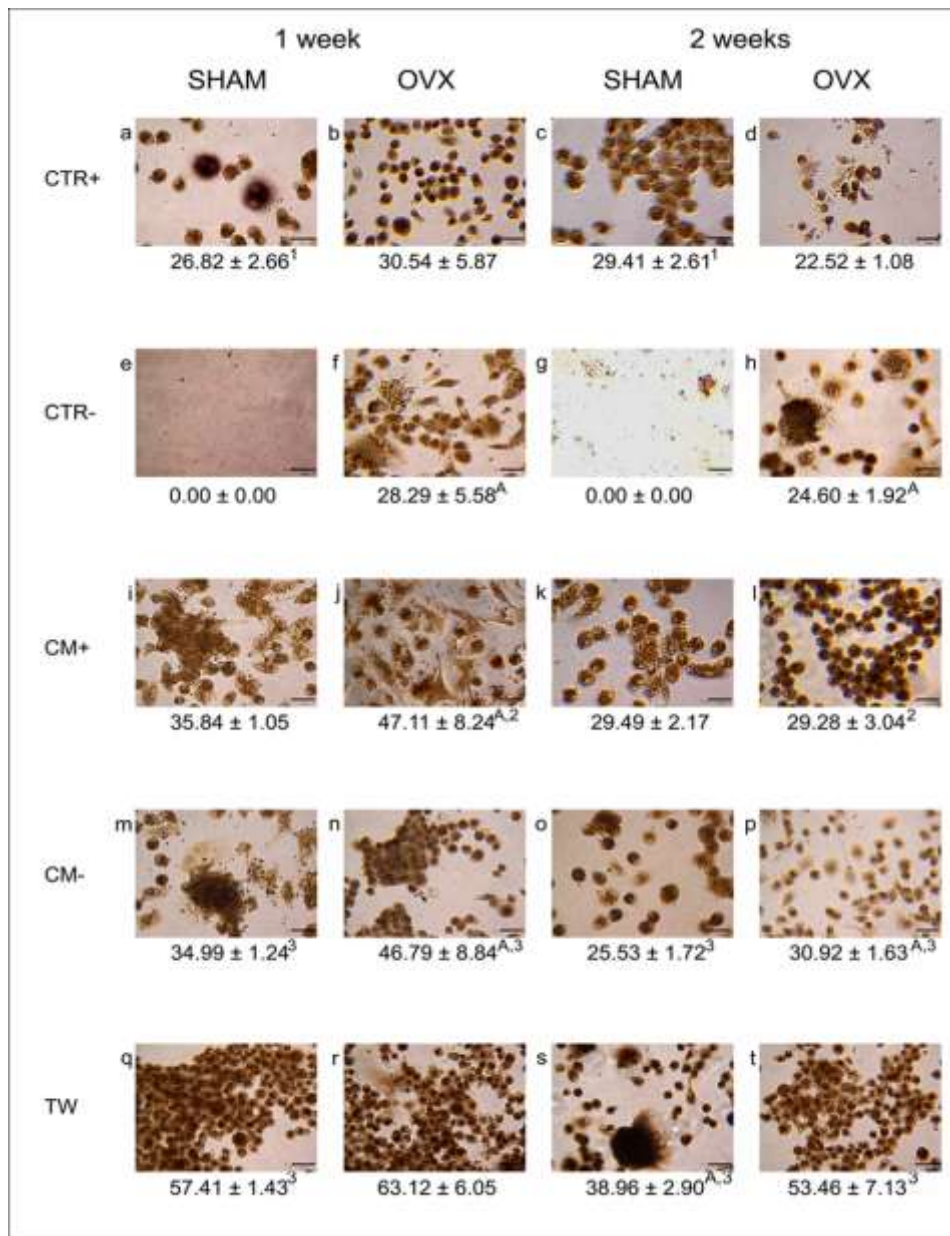


Figure 3.13: TRAP staining images of  $PBMC_{OVX}$  and  $PBMC_{SHAM}$  in CTR-, CTR+, CM-, CM+ and TW culture conditions at one and two weeks.

The osteoporotic condition revealed to have an effect also in terms of number of OCs present in culture, which were counted to be in higher number in CTR+ and CTR- groups of PBMC<sub>OVX</sub>. The evaluation of cytoskeleton network through F-actin labeling did not highlighted appreciable differences between sham and osteoporotic cultures, in which can be visible multinucleated and mature OCs, except for the case of CTR- group of PBMC<sub>SHAM</sub> in which there were not OCs.

As regarding the evaluation of protein contents, the synthesis of CTSK appeared higher in all PBMC<sub>OVX</sub> cultures in comparison to PBMC<sub>SHAM</sub> at every experimental time. The same datum was found for TGF- $\beta$ 1 synthesis, but only for CTR<sup>-</sup> cultures, at both experimental times, and TW cultures, at two weeks, while no difference were found between the others osteoporotic and sham culture conditions. Differently, the evaluation of TNF- $\alpha$  showed in all culture conditions, except for TW one, increased values in osteoporotic groups when compared with sham ones. VEGF synthesis instead seemed to be significantly higher in PBMC<sub>SHAM</sub> than in PBMC<sub>OVX</sub>, in particular in TW group at one week and in CM+ group at both experimental times.

The synthesis of MMPs appeared to be in favor of osteoporotic culture condition, with a higher value of MMP-7 detectable in all groups and experimental times. A similar trend was visible for MMP-9 at the first experimental time, while in the second only CM- and CM+ groups showed values significantly different from sham condition. **(Figure 3.14)**

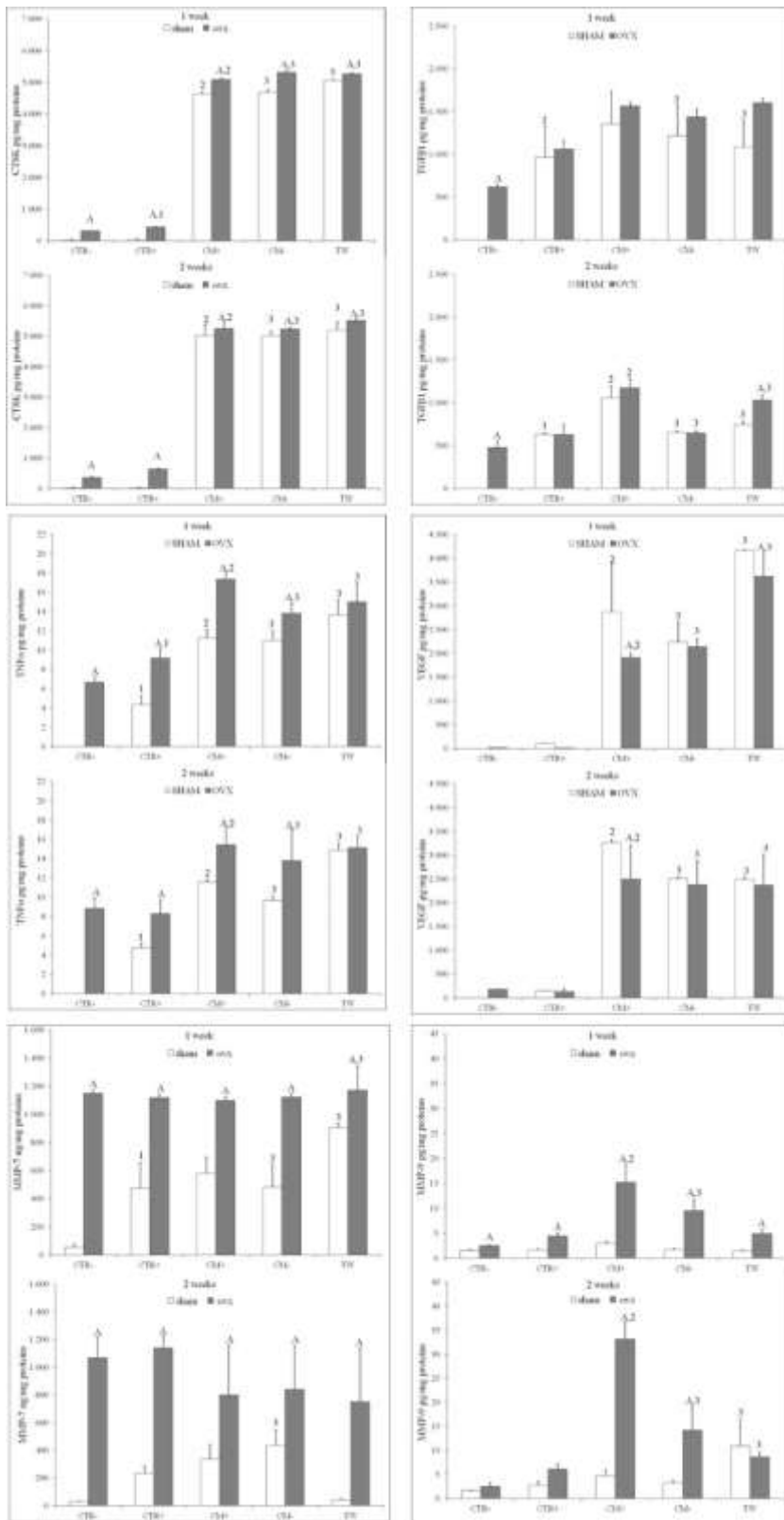


Figure 3.14: Protein content of PBMC<sub>OVX</sub> and PBMC<sub>SHAM</sub> in CTR-, CTR+, CM-, CM+ and TW culture conditions at one and two weeks. [Salamanna et al, 2016]

To deepen the effects that the different present variables had on the performance of the cultures, two specific evaluations were conducted, in particular:

- evaluation of the influence exerted by differentiation factors on PBMC cells (CTR<sup>+</sup> *versus* CTR<sup>-</sup>)
- evaluation of the influence exerted by MRMT-1 conditioned medium in presence of differentiation medium (CM<sup>+</sup> *versus* CTR<sup>+</sup>)
- evaluation of the influence exerted by MRMT-1 conditioned medium and MRMT-1 co-culture system in presence of basal medium (CM<sup>-</sup> and TW *versus* CTR<sup>-</sup>).

The effect of the addition of differentiating factors to cultures revealed to be strongly different between sham and osteoporotic culture, highlighting important difference among the two conditions. In fact, PBMC<sub>SHAM</sub> in culture with differentiating factors (CTR<sup>+</sup> group) showed significantly higher viability and increased values of a number of protein, like CTSK, TGF- $\beta$ 1, TNF- $\alpha$  and MMP-7, aside from a stronger TRAP staining in comparison to the culture with basal medium only, CTR<sup>-</sup>.

Intriguingly, in PBMC<sub>OVX</sub> the absence of differentiating factors seemed not to prevent the differentiation of cells in OCs, so much that no significant different could be find when comparing with CTR<sup>+</sup> group for the same parameters listed previously and for MMP-9 synthesis.

The combination of differentiating factors and MRMT-1 conditioned medium revealed to exert a trophic action on both sham and osteoporotic culture conditions, having a significantly positive effect at all experimental times not only on cells viability but also on the synthesis of CTSK, TNF- $\alpha$  and VEGF, and on TGF- $\beta$  at 2 weeks, while MMP-7 synthesis seemed to be not affected at all.

The main difference between the two conditions was found for TRAP staining and MMP-9 synthesis, which resulted significantly higher in PBMC<sub>OVX</sub> when compared to PBMC<sub>SHAM</sub>.

In the absence of differentiation factors, the effect of MRMT-1 cells, both in the case of conditioned medium (CM-) and co- culture system (TW), was to enhance viability, to strengthen TRAP staining, to increase the synthesis of CTSK, TNF- $\alpha$ , VEGF and TGF- $\beta$ 1 (only at 1 week for PBMC<sub>OVX</sub>) in both sham and osteoporotic conditions.

Taken the two conditions individually, as for PBMC<sub>SHAM</sub>, it could be observed an increased synthesis of MMP-7 when in presence of conditioned medium or co- cultured MTMT-1 while in the case of PBMC<sub>OVX</sub>, in the same experimental groups, it was MMP-9 to be found increased.

### 3.4 Assessment of a 3D Model of Rat Bone Metastases *In Vitro*

The results obtained through Alamar Blue assay showed higher viability in SHAM and OVX rats derived calvaria bone co-cultured with MRMT-1 cells groups in comparison to bone segments cultured alone. At time zero, before dividing samples in the various experimental groups, calvaria segments had comparable viability values, regardless of the provenience from sham or osteoporotic rats. After adding MRMT-1 cells, values of co-cultured groups surged after 7 days, be up to twice the segments culture alone. Viabilities maintained almost stable for all the groups up to 14 days, without any perceptible difference between SHAM and OVX groups. Significant statistical differences were found between SHAM+ MRMT-1 culture and OVX + MRMT-1 culture at each experimental time versus both SHAM and OVX culture alone ( $p < 0.05$ ). (Figure 3.15) (Figure 3.16)

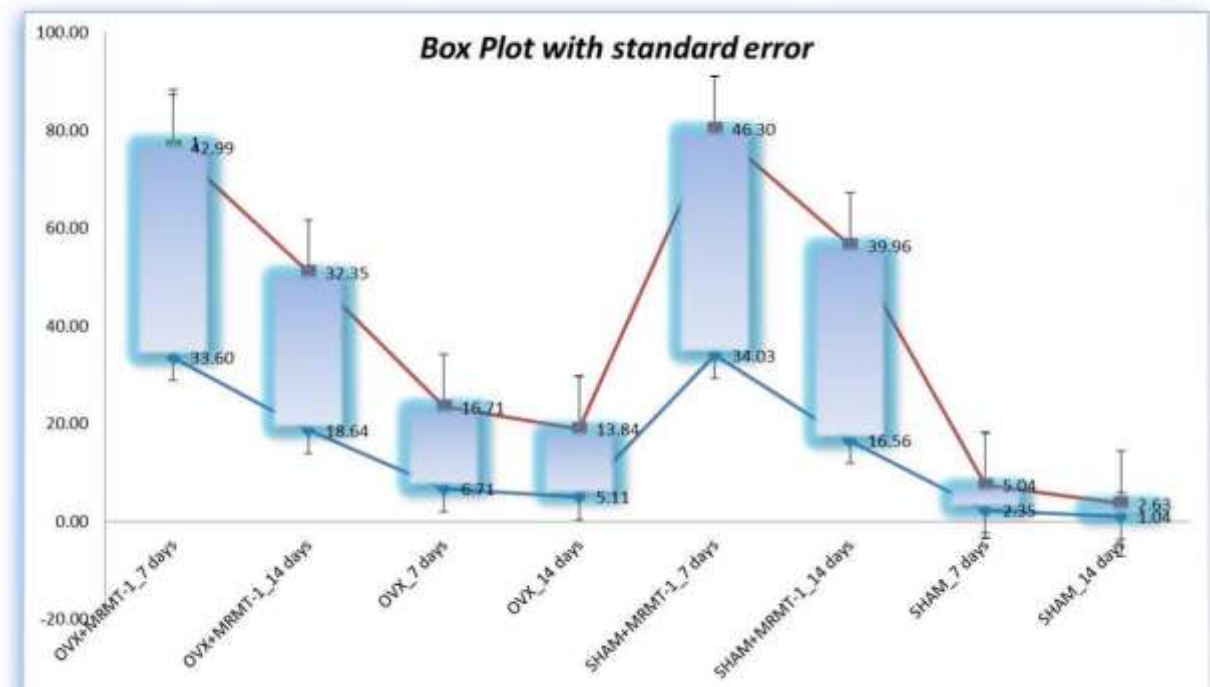


Figure 3.15: Box plot graph of viability values distribution of SHAM, OVX, SHAM+ MRMT-1 and OVX+ MRMT-1 groups at 7 and 14 days of culture.



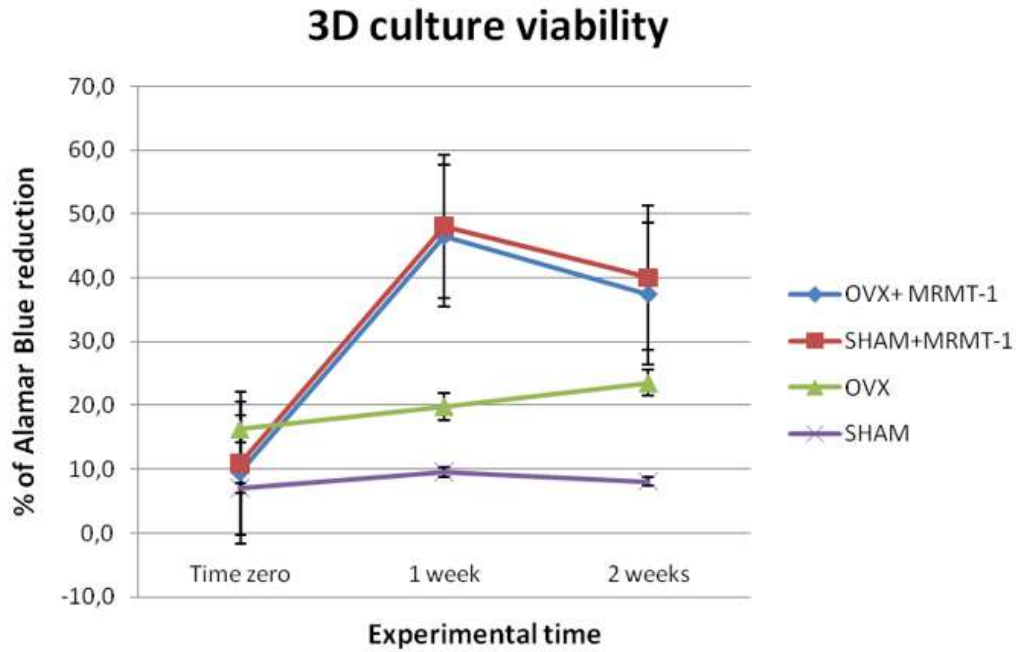


Figure 3.16: Viability trend of SHAM, OVX, SHAM+ MRMT-1 and OVX+ MRMT-1 groups at 7 and 14 days of culture.

The viability evaluation on supernatants from co- cultured groups resulted to be negative, indicating the absence of circulating cells in the culture media and so suggesting that all cancer cells seeded in the same tubes as calvaria segments were attracted to bones and colonized them.

Differently from the course of the culture, analysis of protein expression of MRMT-1 cells co- cultured with bone from different sources revealed intriguing differences between health and osteoporotic condition. In fact, MRMT-1 after 14 days in culture in contact with ovx bone showed an increased phosphorylation of Akt- 473 serine and also a higher expression of Phosphorylated S6 ribosomal (S6RP) protein and Phosphatase and Tensin homolog (p-PTEN) Ser380 in comparison with SHAM co-cultures. Clear signs of boosted feature of aggressiveness in cancer cells cultured in osteoporotic microenvironment in comparison to

the healthy one were given by the increased expression of MMP- 9 and the reduction in E-cadherin expression, both of them classical markers of invasiveness.

The pathways regulating apoptosis proved to be influenced by the presence of OVX bone in terms of decrease in the levels of B-cell lymphoma 2 protein (Bcl2) and contemporary increase of B-cell lymphoma-extra large (Bcl- XL) ones, suggesting a stronger resistance to mechanisms of cellular death in cancer cells. Finally, the ER, usually present in MRMT-1 cells, was still expressed by cells cultured with SHAM calvaria bone segment, but not by cells cultured with OVX bone. (**Figure 3.17**)

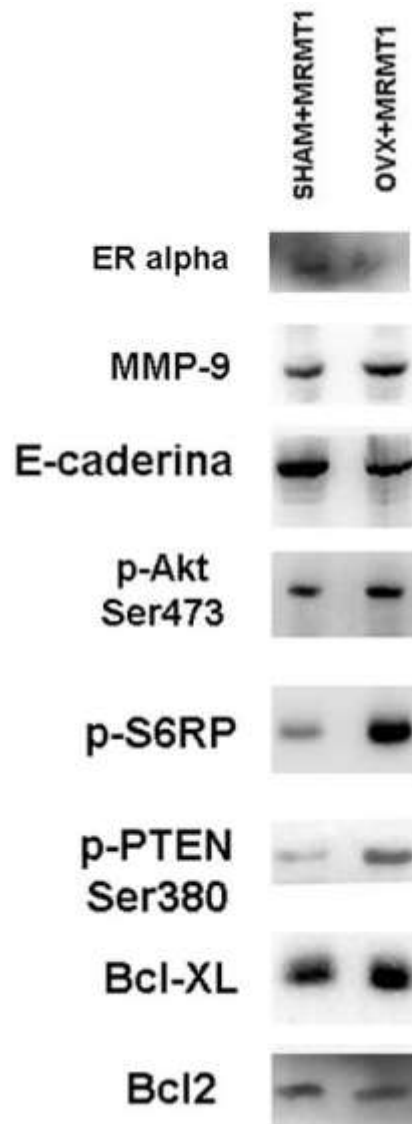


Figure 3.17: Western blot of MRMT-1 protein content after sham and osteoporotic culture

Observation of histological samples highlighted both in SHAM and OVX calvaria bone cultured with MRMT-1 cells the presence of cells, distributed along the line of the periosteum, often grouped in foci, with hyperchromatic and picnotic nuclei. (Figure 3.18)

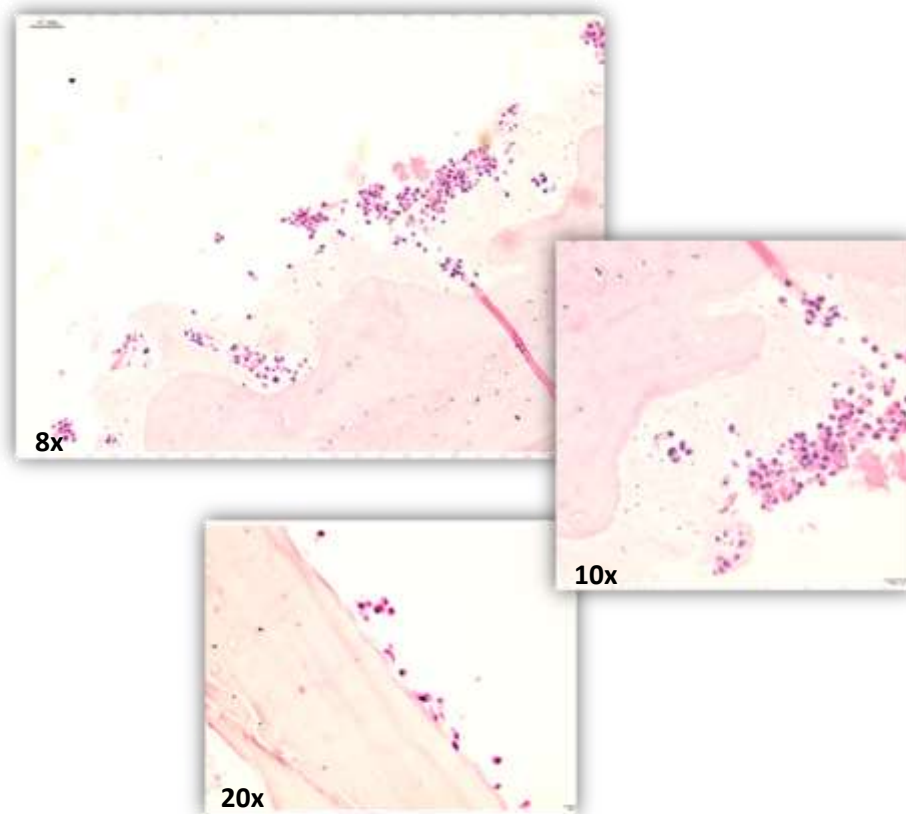


Figure 3.18: Histological images of calvaria segments after culture with MRMT-1 cells, with presence of foci of cancer cells along the periosteum surface. Hematoxylin/Eosin staining.

### 3.5 *In Vivo* Induction of Osteolytic Metastases in osteoporotic rats

Animals survived the surgical procedure and reached the scheduled experimental times without any complications. microPET analysis was performed on all expected animals, without any problems related to the administration of contrast medium or anesthesia required for the execution of the test. At one week after the inoculation of cancer cells, no difference between health and osteoporotic rats could be detectable by microPET analysis. At two weeks, instead, the captation of the radioactive tracer was found to be significantly higher in OVX rats in comparison to SHAM rats ( $p < 0.05$ ). As expected, no difference were found in the controlateral untreated limb in both groups at each experimental times. **(Figure 3.19)**

Macroscopic observation at harvesting of the limbs highlighted, in many animals, the presence of formations around the treated tibias, rounded shaped and dense, that might be tumoral masses, formed probably for the aggressiveness of the used cell line.

Group	Weight (gr)	Glycemia (mg/dl)	Dose (Mbg)
SHAM	214.00 ± 6.09	116.13 ± 21.71	36.71 ± 3.30
OVX	242.33 ± 14.91	113.33 ± 29.11	33.53 ± 5.10

	Group	Averaged	Min	Max	Volume
Right Limb	SHAM	1.28 ± 0.38	0.47 ± 0.40	3.17 ± 1.71	0.55 ± 0.41
	OVX	1.83 ± 0.57	0.49 ± 0.25	5.53 ± 2.48	0.70 ± 0.46
Left Limb	SHAM	0.97 ± 0.26	0.37 ± 0.32	1.51 ± 0.31	0.56 ± 0.41
	OVX	1.07 ± 0.35	0.40 ± 0.22	1.89 ± 0.76	0.62 ± 0.43

Figure 3.19: Biological parameters and microPET analysis results of Sham and Ovx rats



# **CHAPTER 3- DISCUSSION**

The establishment of metastatic disease, intended as the spread and invasion of cells from primary tumour to distant site, still remains the most critical aspect of cancer. Despite the improvement given by early diagnosis, surgical techniques and target therapies, at least 90% of decease among oncologic patients can be ascribable to the presence of advanced metastatic disease. One of the major difficulty in the management of bone metastases is the great biological heterogeneity of cancer cells in the primary and metastatic neoplasia, which can manifests with countless genetic, biological, immunological and biochemical characteristics. *[Awolaran et al, 2016]*

Metastases to bone can be easily reconducted to the so called “epithelial” cancers, like breast and prostate ones; these cells, despite having phenotypic and genotypic characteristics that make them more prone to migrate versus bone, undergo some modification once arrived to the target organs, in order to better adapt and colonize the site. It is so more and more recognized that the microenvironment plays a pivotal role in influencing the establishment of bone metastases and, sometimes, modifying the course of the metastatic disease. Among the various actors taken in consideration, alterations of endocrine status seem to be a promise field of study. It is in fact assessed that androgens and estrogens deprivation lead to important alterations promoting bone loss and osteolysis. The intriguing question, which has not yet been given a satisfactory answer, is if such altered metabolic state can in some ways promote or facilitate establishment of metastases. Many evidence supporting this hypothesis come from literature.

Kraemer et al conducted a study on one hundred and eighty-one women (70 premenopausal, 111 postmenopausal) affected by primary breast cancer, correlating data acquired by quantitative ultrasonometry, performed before adjuvant chemotherapy, and the number of disseminated cells estimated by an harvesting of bone marrow from iliac crest. Results

showed an inverse proportion between BMD and disseminated cancer cells, suggesting that an altered bone status might favor the spread of breast cancer cells. [**Kraemer B et al, 2011**] Ottewell's group found out first in an animal model of androgen deprivation that in condition of low levels of androgens prostate cancer cells invade and grow in bone faster and more aggressively than in animals with a normal endocrine state. The treatment of the animals with Zoledronic acid, an anti-resorptive drug, leads to a reduction in tumor growth, suggesting a mechanism driven by enhanced OCs activity. [**Ottewell PD et al, 2014**] By the way, not many certainties have been made on this topic and the most of the study on the subject employed *in vivo* model, usually xenogenic, or refers to clinical evidence.

A considerable drawback in the study of bone metastases is the great complexity in the setting of *in vitro* models which might be reliable and sufficiently similar to the clinical situation. Undeniably, in the research on metastatic disease, *in vitro* models have always played a crucial role. Probably the first paper that can be identified on this topic dates back to 1967 and through an *in vitro* study identified some evidence of neoplastic conversion. [**Sanford KK et al, 1967**] Since then, many progress have been done in the field of *in vitro* models and, most importantly, many milestones in the knowledge of the metastatic story have been reached. The use of experimental set-up nowadays of common use in biological laboratory, such as bidimensional direct co-cultures, cultures with transwell or conditioned medium, have helped to find out evidence on the tropism of primary cancer cells for bone, dormancy and invasion of disseminated cells and on the interaction with bone cell populations. [**Arrigoni C et al, 2016**] A greater level of complexity, however, need to be reached to deepen enough mechanisms underlying the relationship between cancer and bone. In fact, bone microenvironment is a varied and heterogeneous world in which too many factors- resident cells, namely OBs, OCs, MSCs, vascular supply, oxygen levels- are present to not to be taken into account and considered in the set up of an *in vitro* study. Also the most



recent developments, like use of bioreactors, microfluidic systems or natural/synthetic matrices, seem to suffer from some limitations. On the one hand, they allow to use contemporary different types of cells and to study their interaction, also in terms of migration and capability to remodel matrix, with the possibility to control the environment biochemically and biophysically and to recreate a microvascular network. On the other hand, however, these systems can lack of reproducibility, require too long times for culture or, on the contrary, can be carried on for a too short time, and they can often not be able to reproduce faithfully the native bone microenvironment. [*Salamanna et al, 2016* ]

In the light of these considerations, the use of model of direct contact between bone and cancer cells could seem to be preferable, allowing to obtain the closest condition to native microenvironment. In addition, beside the evaluation of bone colonization, which still remains the most studied aspect of metastatic disease through 3D model, this type of culture allows to study quite easily the mutual interaction between bone and cells.

*Curtin et al* developed a tridimensional xenogenic model co-culturing mice calvaria bone with breast cancer cell lines, MCF-7 and MDA-MB-231, and prostate tumor cell lines, LnCap Clone FGC and PC-3, showing that it could be applied for the study of bone alteration due to biochemical or chemical changes in the environment or for the presence of tumor cells. [*Curtin et al, 2012*]

This model was then regained and modified by *Salamanna et al*, using human male and female bone tissue co-cultured with MCF7 and PC-3 cells. Authors deeply investigated bone colonization from cancer cells, highlighting the marked tropism secondary to species and sex. [*Salamanna et al, 2016*] Subsequently, the same group used the model to assess the influence of OP on migration of breast cancer cells to bone, assessing a greater attraction of cells versus bone harvested from osteoporotic patients in comparison to healthy ones. [*Salamanna et al, 2016*]

It is not so easy to find in literature 3D bone tissue models, not only for application in the oncologic field but also for study of regenerative medicine. The models of calvaria segments and femoral condyles proposed aimed at evaluating the possibility to keep in culture two very different type of bone- flat bone and trabecular bone- for a period of time that could be reasonable in the perspective of many kind of evaluations. Both cultures proved to be able to preserve viability and metabolism of bone segments, and also that experimental times did not affect bone structure. These evidences have already opened up the possibility to apply the femoral condyle model for evaluations of biocompatibility of new biomaterials and the assessment of *in vitro* model for the study of pathology like osteonecrosis (*unpublished data*). Calvaria bone culture instead appeared to be more suitable for the set-up of 3D model of metastases in a compromised bone. The selection of a flat bone could seem unconventional, as usually thinking about bone metastases in another target district, such as femur or vertebra for example. Actually, calvaria bone, even osteoporotic, is fairly described in literature for studies on evaluation of bone formation and repair of cranial defects (*Scalize et al, 2015; Hirata et al, 2015*). Beside the “technical” reason, or else related to the possibility to better isolate and evaluate cancer cells from a flat bone in comparison to the others, the choice revealed to be successful also because it could be demonstrated that, being OP a systemic disease, any type of bone, taken from any part of the body, exerts the same effect on cancer cells.

One the more evident lacuna in many study about metastatic progression to bone is the analysis of how and to what extent bone microenvironment influences and alters the genotype and phenotype of cancer cells, in particular if disseminated cells arrive to an already compromised bone for the connivance of oncologic state with other conditions like OP.

In order to perform this analysis, a characterization of MRMT-1 cell line became mandatory. These rat breast cancer cells in fact proved to be very aggressive and effective in inducing, in

an allogenic animal model, the formation of osteolytic lesions, very similar to those that are found in patients affected by bone metastases [*Fini et al, 2013*] but they were still poorly characterized. The evaluations conducted substantially confirmed these previous indications, by returning the view of a very aggressive cell line, as underlined by the presence of classical characteristics, like suppression of p53 and activated pathway of PI3K/AK/mTOR, reducing apoptosis and allowing unregulated cell growth. Very interestingly, when co-cultured with bone from different sources, MRMT-1 demonstrated to undergo modifications according to the kind of bone- osteoporotic or healthy. Activity of Akt is one of the classical evaluation in the study of cancer, being frequently altered in case of establishment of tumor. [*Vincent et al, 2011*] Usually, phosphorylation on Ser473 is considered a reliable indicator of the activation of this pathway and it has been correlated with poor outcome in breast cancer [*Dai et al, 2005*]. On the bases of the results obtained from calvaria culture, the osteoporotic microenvironment proved to increase Akt phosphorylation on Ser473, which suggests a stronger survival of cells, among the push to growth and a higher metabolic activity. The activation of Akt pathway usually finds its negative feedback in the PI(3,4,5)P<sub>3</sub> phosphatase, PTEN. In cells cultured with OVX bone can be observed a greater phosphorylation of p-PTEN on Ser380, mechanism which have already been proved to be involved in the onset of other type of cancer, like gastric tumors. [*Yang et a, 2013*]

Further confirmation arrives from increasing of MMP- 9 expression, the reduction of E-cadherin, both classical markers of invasiveness, and the reduction of Bcl-2 and the simultaneous increase of Bcl-XL, clear mechanisms present in cancer for inhibition of apoptosis. One of the most intriguing aspect, which surely needs further investigations, seem to remain the loss of ER, expressed by the cell line after culture with healthy bone, but no more present in the cells cultured with osteoporotic bone. It has already been described in literature a relationship between loss of ERs and metastatic phenotype of cancer cells. In

particular, some papers suggest that silencing ERs gene in MCF-7 breast cancer cells stimulates the expression of genes related to cell migration and promoting the onset of metastatic disease, also via inducing EMT of cancer cells. [Saleh et al, 2011]

These findings serve as backdrop to the study conducted co-culturing MRMT-1 cells with osteoporotic OCs. In that case, the evaluation was on the contrary about the effect that tumor cells exerted on OCs in healthy and osteoporotic condition and, even under this point of view, the most significant data came from the osteoporotic condition. OVX OCs are more sensitive to the action of breast cancer cells, and exhibit a more pronounced viability and activity.

The obtained results underline the complex and mutual influence of the tumor cells with the cells of the bone tissue, supporting the hypothesis that the presence of a condition of altered bone metabolism, such as OP, promotes the development and metastatic progression, and this “fatal attraction” between osteoporotic bone and breast cancer cells creates an endless loop. In fact, this mechanism finds expression in a double, specular way, that is on the one hand increasing the phenotypic characteristics of aggressiveness and invasiveness of tumor cells and, on the other hand, stimulating OCs to enhance their osteolytic activity and so further impoverishing an already altered bone, activating a series of events which even more favor cell colonization.

The success of the 3D *in vitro* model used for the study marks a point in favor of the culture model of direct contact between bone and tumor cells, giving good prospects of application also for the study of other kind of cancers with different tissues. The model might help not only in the deepening of understanding of the mechanisms driving the metastatic journey, but also for detecting molecules or pathways that can be targeted for the treatment of bone metastases. More stimulating, in the light of the emerged role of OP, it could be interesting to find out new methods for early diagnosis of impaired bone condition and to initiate screening programs to better prevent and manage the complications related to the connivance of the two

pathologies. Finally, the set-up of new and more and more reliable *in vitro* models fits perfectly in the fulfillment of the principle of the 3R (Replacement, Reduction and Refinement) for animal testing, whose addressing is an increasingly strong need. Despite *in vivo* models can't be yet completely replaced, in the light of the complexity of biological and systemic response of a whole organism, the assessment of *in vitro* model able to mimic physiological state as better as possible is an essential mean, testing preventively treatment and therapies and selecting only the most promising ones, in order to reduce and optimize the use of animals. If the histological and immunohistochemical assessments on *in vivo* model conducted will confirm data obtained from PET imaging, the proposed advanced 3D model might be employed at least in the initial steps of research for the study of the etiopathogenesis and treatment of bone metastases.

# References

- **Adachi T, Aonuma Y, Ito S., Tanaka M, Hojo M, Takano-Yamamoto T and Kamioka H.** “*Osteocyte calcium signaling response to bone matrix deformation*”. J Biomech, 2009; 42: 2507-2512.
- **Adachi T, Aonuma Y, Tanaka M, Hojo M, Takano-Yamamoto T and Kamioka H.** “*Calcium response in a single osteocyte to locally applied mechanical stimulus: differences in cell process and cell body*”. J Biomech, 2009; 42: 1989-1995.
- **Albright F, Bloomberg E, Smith PH.** “*Postmenopausal osteoporosis*”. Trans. Assoc. Am. Physicians. 1940; 55:298–305.
- **Arnett T.** “*Regulation of bone cell function by acid- base balance*”. Proc Nutr Soc, 2003; 62: 511-520.
- **Arrigoni C, Bersini S, Gilardi M, Moretti M.** “*In Vitro Co-Culture Models of Breast Cancer Metastatic Progression towards Bone*”. Int J Mol Sci. 2016 Aug 25;17(9). pii: E1405. doi: 10.3390/ijms17091405.
- **Awolaran O, Brooks SA, Lavender V.** “*Breast cancer osteomimicry and its role in bone specific metastasis; an integrative, systematic review of preclinical evidence*”. The Breast 30 (2016) 156e171
- **Bellavia D, Costa V, De Luca A, Maglio M, Pagani S, Fini M, Giavaresi G.** “*Vitamin D Level Between Calcium-Phosphorus Homeostasis and Immune System: New Perspective in Osteoporosis*”. Curr Osteoporos Rep. 2016 Oct 13.
- **Buijs JT and van dr Pluijm G.** “*Osteotropic cancers: From primary tumor to bone.*” Cancer Lett, 2009; 2: 177-193.

- **Chen YC, Sosnoski DM and Mastro AM.** „*Breast cancer metastasis to the bone: mechanism of bone loss*”. *Breast Cancer Res*, 2010; 12: 215-225.
- **Coleman RE.** “*Metastatic bone disease: clinical features, pathophysiology and treatment strategies*”. *Cancer Treat Rev*, 2001; 27: 165-17.
- **Coleman RE, Lipton A, Roodman GD, Guise TA, Boyce BF, Brufsky AM, Clézardin P, Croucher PI, Gralow GR, Hadji P, Holen I, Mundy GR, Smith MR and Suva LJ.** “*Metastasis and bone loss: advancing treatment and prevention*”. *Cancer Treat. Rev*, 2010; 36: 615-620.
- **Curtin P, Youm H, Salih E.** “*Three-dimensional cancer-bone metastasis model using ex-vivo co-cultures of live calvarial bones and cancer cells*”. *Biomaterials*. 2012 Feb;33(4):1065-78. doi: 10.1016/j.biomaterials.2011.10.046. Epub 2011 Nov 8.
- **Dai DL, Martinka M and Li GJ.** “*Prognostic Significance of Activated Akt Expression in Melanoma: A Clinicopathologic Study of 292 Cases*”. *Clin Oncol* 23:1473-1482.
- **Eiksen EF.** “*Cellular mechanisms of bone remodeling*”. *Rev Endocr Metab Disord*. 2010; 11:219–227
- **Faienza MF, Ventura A, Marzano F, Cavallo L.** “*Postmenopausal osteoporosis: the role of immune system cells*”. *Clin Dev Immunol*. 2013; 2013:575936. doi: 10.1155/2013/575936. Epub 2013 May 23.
- **Fini M, Salamanna F, Veronesi F, Torricelli P, Nicolini A, Benedicenti S, Carpi A, Giavaresi G.** “*Role of obesity, alcohol and smoking on bone health*”. *Front Biosci (Elite Ed)*. 2012 Jun 1; 4:2686-706.
- **Fini M, Salamanna F, Parrilli A, Martini L, Cadossi M, Maglio M, Borsari V.** “*Electrochemotherapy is effective in the treatment of rat bone metastases*”. *Clin Exp*

Metastasis. 2013 Dec;30(8):1033-45. doi: 10.1007/s10585-013-9601-x. Epub 2013 Jul 7

- **Frost HM.** “*Tetracycline-based histological analysis of bone remodeling*”. *Calcif Tissue Res.* 1969;3(3):211-37
- **Gatenby RA, Gawlinski ET, Gmitro AF, Kaylor B and Gillies RJ.** “*Acid-Mediated Tumor Invasion: a Multidisciplinary Study*”. *Cancer Res*, 2006; 66: 5216-5223.
- **Gupta GP and Massagué J.** “*Cancer Metastasis: Building a Framework*”. *Cell*, 2006; 127: 679-694.
- **Hadjidakis JH and Androulakis II.** “*Bone Remodeling*”. *Ann. N.Y. Acad. Sci.* 1092: 385–396 (2006). doi: 10.1196/annals.1365.035
- **Hansen MF, Seton M and Merchant A.** “*Osteosarcoma in Paget's Disease of Bone*”. *J Bone Min Res*, 2007; 21: 58-63.
- **Henriksen K, Neutzsky-Wulff AV, Bonewald LF and Karsdal MA.** “*Local communication on and within bone controls bone remodeling*”. *Bone*, 2009; 44: 1026-1033
- **Hirata HH, Munhoz MAS, Plepis AMG, Martins VCA, Santos GR, Galdeano EA.** “*Feasibility study of collagen membranes derived from bovine pericardium and intestinal serosa for the repair of cranial defects in ovariectomised rats*”. *Cunha. Injury, Int. J. Care Injured* 46 (2015) 1215–1222
- **Hu K and Olsen BR.** “*The roles of vascular endothelial growth factor in bone repair and regeneration*”. *Bone* 91 (2016) 30–38
- **Imai Y, Kondoh S, Kouzmenko A and Kato S.** “*Minireview: Osteoprotective Action of Estrogens Is Mediated by Osteoclastic Estrogen Receptor- $\alpha$* ”. *Mol Endocrinol*, May 2010, 24(5):877–885



- **Kan C, Vargas G, Le Pape F and Clézardin P.** “*Cancer Cell Colonisation in the Bone Microenvironment*”. Int. J. Mol. Sci. 2016, 17, 1674; doi:10.3390/ijms17101674.
- **Kaplan RN, Riba RD, Zacharoulis S, Bramley AH, Vincent L, Costa C, MacDonald DD, Jin DK, Shido K, Kerns SA, Zhu Z, Hicklin D, Wu Y, Port JL, Altoeki N, Port ER, Ruggero D, Shmelkov SV, Jensen KK, Rafii S and Lyden D.** “*VEGFR1- positive haematopoietic bone marrow progenitors initiate the pre-metastatic niche*”. Nature, 2005; 438: 820-827.
- **Kaplan RN, Psaila B and Lyden D.** “*Bone marrow cells in the “pre- metastatic niche: within bone and beyond*”. Cancer Metastasis Rev, 2006; 25: 521-529
- **Khosla S.** “*Minireview: The OPG/RANKL/RANK System*”. Endocrinology, 2001; 142: 5050-5055.
- **Kingsley LA, Fournier PGJ, Chirwin JM and Guise TA.** “*Molecular Biology of Bone Metastasis*”. Mol Cancer Ther, 2007; 6: 2609-2617
- **Kozlow W and Guise TA.** “*Breast cancer metastasis to bone: mechanisms of osteolysis and implications for therapy*”. J Mammary Gland Biol Neoplasia 2005;10(2):169–80.
- **Kraemer B, Rothmund R, Banys M, Krawczyk N, Solomayer E-F, Mack C, Wallwiener D and Fehm T.** “*Impaired Bone Microenvironment: Correlation between Bone Density and Presence of Disseminated Tumor Cells*”. Anticancer Research 31: 4423-4428 (2011)
- **Le Gall C, Bellahcène A, Bonnelye E, Gasser JA, Castronovo V, Green J, Zimmermann J and Clézardin P.** “*A cathepsin K inhibitor reduces breast cancer induced osteolysis and skeletal tumor burden*”. Cancer Res, 2007; 67: 9894-9902.

- **Ooi LL, Zheng Y, Stalgis-Bilinski K, Dunstan CR.** “*The bone remodeling environment is a factor in breast cancer bone metastasis*”. Bone 48 (2011) 66–70
- **Ottewell PD, Brown HK, Jones M, Rogers TL, Cross SS, Brown NJ, Coleman RE, Holen I.** “*Combination therapy inhibits development and progression of mammary tumours in immunocompetent mice*”. Breast Cancer Res Treat. 2012 Jun;133(2):523-36. doi: 10.1007/s10549-011-1782-x. Epub 2011 Sep 29.
- **Ottewell PD, Wang N, Brown HK, Reeves KJ, Fowles CA, Croucher PI, Eaton CL and Holen I.** “*Zoledronic acid has differential anti-tumour activity in the preand post-menopausal bone microenvironment in vivo*”. Clin Cancer Res. 2014 June 1; 20(11): 2922–2932. doi:10.1158/1078-0432. CCR-13-1246.
- **Pagani S, Fini M, Giavaresi G, Salamanna F, Borsari V.** “*The active role of osteoporosis in the interaction between osteoblasts and bone metastases*”. Histol Histopathol. 2016 Jan;31(1):83-93. doi: 10.14670/HH-11-651. Epub 2015 Aug 7.
- **Paget S.** “*The distribution of secondary growths in cancer of the breast*”. Lancet 1889; 133: 3.
- **Raisz LG.** “*Physiology and Pathophysiology of Bone Remodeling*”. Clin Chem, 1999; 45: 1353-1358
- **Reid IR.** “*Relationships between fat and bone.* Osteoporos Int 2008;19(5): 595–606.
- **Riggs BL, Melton LJ.** “*Evidence for two distinct syndromes of involutinal osteoporosis*”. 3rd Am J Med. 1983 Dec; 75(6):899-901.
- **Roodman GD.** “*Mechanism of Bone Metastasis*”. N Engl J Med, 2004; 350: 1655-1664.
- **Rose AAN and Siegel PM.** “*Breast Cancer- derived factors facilitate osteolytic bone metastasis*”. Bull Cancer, 2006; 93: 931-943.

- **Ryu J, Kim HJ, Chang EJ, Huang H, Banno Y, Kim HH.** “*Sphingosine 1-phosphate as a regulator of osteoclast differentiation and osteoclast-osteoblast coupling*”. EMBO J. 2006; 25:5840– 51.
- **Salamanna F, Maglio M, Giavaresi G, Pagani S, Giardino R, Fini M.** “*In vitro method for the screening and monitoring of estrogen-deficiency osteoporosis by targeting peripheral circulating monocytes*”. Age (Dordr). 2015 Aug;37(4):9819. doi: 10.1007/s11357-015-9819-4. Epub 2015 Aug 7.
- **Salamanna F, Pagani S, Maglio M, Borsari V, Giavaresi G, Martelli AM, Buontempo F, Fini M.** “*Estrogen-deficient osteoporosis enhances the recruitment and activity of osteoclasts by breast cancer cells*”. Histol Histopathol. 2016 Jan;31(1):83-93. doi: 10.14670/HH-11-651. Epub 2015 Aug 7.
- **Salamanna F, Contartese D, Maglio M, Fini M.** “*A systematic review on in vitro 3D bone metastases models: A new horizon to recapitulate the native clinical scenario?*” Oncotarget. 2016 Jul 12;7(28):44803-44820. doi: 10.18632/oncotarget.8394.
- **Salamanna F, Borsari V, Brogini S, Giavaresi G, Parrilli A, Cepollaro S, Cadossi M, Martini L, Mazzotti A, Fini M.** “*An in vitro 3D bone metastasis model by using a human bone tissue culture and human sex-related cancer cells*”. Oncotarget. 2016 Nov 22;7(47):76966-76983. doi: 10.18632/oncotarget.12763.
- **Salamanna F, Borsari V, Brogini S, Torricelli P, Cepollaro S, Cadossi M, Fini M.** “*A Human 3D In Vitro Model to Assess the Relationship Between Osteoporosis and Dissemination to Bone of Breast Cancer Tumor Cells*”. J Cell Physiol. 2016 Dec 7. doi: 10.1002/jcp.25708. [Epub ahead of print]
- **Saleh SA, Mulla FA, Luqmani YA.** “*Estrogen Receptor Silencing Induces Epithelial to Mesenchymal Transition in Human Breast Cancer Cells*”. PLoS ONE 6(6): e20610. doi:10.1371/journal.pone.0020610

- **Sanford KK, Barker BE, Woods MW, Parshad R, Law LW.** “*Search for "indicators" of neoplastic conversion in vitro*”. J Natl Cancer Inst. 1967 Oct;39(4):705-33.
- **Scalize PH, de Sousa1 LG, Hallak Regalo SC, Semprini M, Pitol1 DL, da Silva GA, de Almeida Coelho J, Coppi AA, Lobo Laad AA, Fittipaldi Bombonato Prado K and Siessere S.** “*Low-level laser therapy improves bone formation: stereology findings for osteoporosis in rat model*”. Lasers Med Sci (2015) 30:1599–1607 DOI 10.1007/s10103-015-1773-y
- **Schapira D and Schapira C.** “*Osteoporosis: the evolution of a scientific term*”. Osteoporos Int. 1992 Jul;2(4):164-7.
- **Schipani E, Maes C, Carmeliet G, Semenzaet GL.** “*Regulation of Osteogenesis-Angiogenesis Coupling*”. JBMR. Volume 24, Number 8, 2009. Published online on June 29, 2009; doi: 10.1359/JBMR.090602
- **Shemanko CS, Cong Y and Forsyth A.** “*What Is Breast in the Bone?*”. Int. J. Mol. Sci. 2016, 17, 1764; doi:10.3390/ijms17101764
- **Tamura D, Hiraga T, Myoui A, Yoshikawa H and Yoneda T.** “*Cadherin- 11-mediated interactions with bone marrow stromal/osteoblastic cells support selective colonization of breast cancer cells in bone*”. Int J Oncol, 2008; 33: 17-24
- **Vincent EE, Elder DJE, Thomas EC, Phillips L, Morgan C, Pawade J, Sohail M, May MT, Hetzel MR and Tavare JM.** “*Akt phosphorylation on Thr308 but not on Ser473 correlates with Akt protein kinase activity in human non-small cell lung cancer*”. British Journal of Cancer (2011) 104, 1755 – 1761.
- **Wright LE and Guise TA.** “*The Microenvironment Matters: Estrogen Deficiency Fuels Cancer Bone Metastases*” Clin Cancer Res. 2014 June 1; 20(11): 2817–2819. doi:10.1158/1078-0432. CCR-14-0576.

- **Wua Y, Chen W, Xu S, Zhang N.** “*Osteoporosis as a potential contributor to the bone metastases*”. *Medical Hypotheses* 75 (2010) 514–516
- **Yin JJ, Pollock CB and Kelly K.** “*Mechanism of cancer metastasis to bone*”. *Cell Res*, 2005; 15: 57-62.
- **Yanga Z, Yuana X, Chena J, Luoa S, Luoc Z, Lu N.** “*Reduced expression of PTEN and increased PTEN phosphorylation at residue Ser380 in gastric cancer tissues: A novel mechanism of PTEN inactivation*”. *Clinics and Research in Hepatology and Gastroenterology* (2013) 37, 72—79
- **Zaman G, Jessop HL, Muzylak M, De Souza RL, Pitsillides AA, Price JS, Lanyon LL.** “*Osteocytes use estrogen receptor alpha to respond to strain but their ERalpha content is regulated by estrogen*”. *J Bone Miner Res*. 2006 Aug;21(8):1297-306.